**T.R.**
**ONDOKUZ MAYIS UNIVERSITY**
**INSTITUTE OF GRADUATE STUDIES**
**DEPARTMENT OF NANOSCIENCE AND NANOTECHNOLOGY**

# SYNTHESIS AND CHARACTERIZATION OF CHITOSAN/POLY(VINYLALCOHOL)/POLY(VINYLPYRROLIDONE) HYDROGELS FOR BIOMEDICAL APPLICATION

Master's Thesis

**Batool AL-MAFRACHI**

Supervisor

**Prof. Dr. Ömer ANDAÇ**

This thesis was supported by Ondokuz Mayıs University with project number PYO.FEN.1904.22.008

**SAMSUN**

2023

## DECLARATION OF COMPLIANCE WITH SCIENTIFIC ETHIC

I hereby declare and undertake that I complied with scientific ethics and academic rules in all stages of my Master's Thesis, that I have referred to each quotation that I use directly or indirectly in the study, and that the works I have used consist of those shown in the sources, that it was written in accordance with the institute writing guide and that the situations stated in the article 3, section 9 of the Regulation for TÜBİTAK Research and Publication Ethics Board were not violated.

Is Ethics Committee Necessary?

Yes ☐ (If it necessary, please add appendices.)

No ☒

25/05/2023

Batool AL-MAFRACHI

## DECLARATION OF THE THESIS STUDY ORIGINALITY REPORT

**Thesis Title :** SYNTHESIS AND CHARACTERIZATION OF CHITOSAN/POLY(VINYLALCOHOL)/POLY(VINYLPYRROLIDONE) HYDROGELS FOR BIOMEDICAL APPLICATION

As a result of the originality report taken by me from the plagiarism detection program on 24 /05 /2023 for the thesis titled above;

Similarity ratio : % 18

Single resource rate : % 2 has been released.

25/05/2023

Prof. Dr. Ömer ANDAÇ

# ÖZET


BİYOMEDİKAL UYGULAMALAR İÇİN
KİTOSAN/POLİVİNİLALKOL/POLİVİNİLPROLİDEN HİDROJELLERİN
SENTEZİ VE KARAKTERİZASYONU

Batool AL-MAFRACHI
Ondokuz Mayıs Üniversitesi
Lisansüstü Eğitim Enstitüsü
Nanobilim ve Nanoteknoloji Ana Bilim Dalı
Yüksek Lisans, Haziran/2023
Danışman: Prof. Dr. Ömer ANDAÇ

Bu çalışma, dolgu maddesi olarak kitosan, polivinil alkol (PVA), polivinilpirolidon (PVP) ve nano-hidroksiapatit (nHA) içeren biyomedikal uygulamalar için yeni bir biyouyumlu hidrojel filmin sentezine odaklanmaktadır. Amaç, nHA'nın polimerik matris üzerindeki etkisini ve hidrojel filmin biyomedikal uygulamalardaki potansiyelini araştırmaktır.

Hidrojel filmler, bir çözelti döküm tekniği kullanılarak hazırlandı. 20 °C'de %1 sulu asetik asit içinde %1.75 kitosan, 80°C'de damıtılmış su içinde %1 PVA ve %2 PVP çözeltileri birlikte karıştırıldı ve ardından değişen oranlarda nHA eklendi.

Hazırlanan hidrojel film numuneleri termogravimetrik analizler (TGA), diferansiyel tarama kalorimetrisi (DSC), taramalı elektron mikroskobu (SEM), antibakteriyel aktivite testi, Fourier dönüşümü kızılötesi (FTIR) spektroskopisi, mekanik testler ve şişme analizi gibi çeşitli karakterizasyonlara tabi tutuldu ve ilaç salım çalışmaları yapıldı.

Hidrojel film, antibakteriyel özellikleri artıran nHA'nın dahil edilmesiyle, özellikle Gram-pozitif bakterilere karşı mükemmel antibakteriyel davranış sergiledi. TGA sonuçları, bozunma aşamaları sırasındaki ağırlık kaybı yüzdesinin, nHA içeren hidrojel filmlerde içermeyenlere kıyasla daha düşük olduğunu gösterdi. FTIR spektrumları, hidrojelin moleküler yapısının nHA'nın dahil edilmesinden minimum düzeyde etkilendiğini ortaya koydu. Hidrojel filmlerin şişme davranışının nHA miktarına bağlı olarak değiştiği gözlendi. İlaç salım profili, hızlı salım ve iyi stabilite gösterdi. Filmlere nHA eklenmesi, kuvveti ve kopmadaki uzamayı arttırdı, bu da geliştirilmiş mekanik mukavemet ve sünekliği artışı sağladı. Ancak Young modülünü düşürerek filmleri daha yumuşak veya daha az sert hale getirdi. Polimerik hidrojel filmin nHA ile kombinasyonu, biyomedikal uygulamalar için umut verici bir potansiyel göstermektedir. Biyomedikal alanlarda tam potansiyelini keşfetmek için daha fazla araştırmaya ihtiyaç vardır.



**Anahtar Kelimeler:** Kitosan; Polivinil alkol; Polivinilpirolidon; nano-hidroksiapatit; biyolojik olarak uyumlu; hidrojel; İlaç salınımı

# ABSTRACT

SYNTHESIS AND CHARACTERIZATION OF CHITOSAN/POLY(VINYLALCOHOL)/POLY(VINYLPYRROLIDONE) HYDROGELS FOR BIOMEDICAL APPLICATION

Batool AL-MAFRACHI
Ondokuz Mayıs University
Institute of Graduate Studies
Department of Nanoscience and Nanotechnology
Master, June /2023
Supervisor: Prof. Dr. Ömer ANDAÇ

This work focuses on the synthesis of a novel biocompatible hydrogel film for biomedical applications, incorporating chitosan, polyvinyl alcohol (PVA), polyvinylpyrrolidone (PVP), and nano-hydroxyapatite (nHA) as a filler. The aim is to investigate the effect of nHA on the polymeric matrix and explore the potential of the hydrogel film in biomedical applications.

The hydrogel films were prepared using a solution-casting technique. Solutions of 1.75% chitosan in 1% aqueous acetic acid at 20 °C, 1% PVA, and 2% PVP in distilled water at 80°C were mixed together, followed by the addition of varying ratios of nHA.

The prepared hydrogel film samples were subjected to various characterizations, including thermogravimetric analyses (TGA), differential scanning calorimetry (DSC), scanning electron microscopy (SEM), antibacterial activity testing, Fourier transform infrared (FTIR) spectroscopy, mechanical testing, swelling analysis, and drug release profiling.

The hydrogel film exhibited excellent antibacterial behavior, particularly against Gram-positive bacteria, with the incorporation of nHA enhancing the antibacterial properties. TGA results showed that the weight loss percentage during degradation stages was lower in hydrogel films containing nHA compared to those without. FTIR spectra indicated that the molecular structure of the hydrogel was minimally affected by the incorporation of nHA. The swelling behavior of the hydrogel films was influenced by the quantity of nHA incorporated. The drug release profile demonstrated rapid release and good stability. The addition of nHA to the films increases the force and elongation at break, indicating improved mechanical strength and ductility. However, it decreases Young's modulus, making the films softer or less stiff. The combination of the polymeric hydrogel film with nHA shows promising potential for biomedical applications. Further research is needed to explore its full potential in biomedical fields.

**Keywords:** Chitosan; Polyvinylalcohol; Polyvinylpyrrolidone; nano-hydroxyapatite; Biocombatiable; Hydrogel; Drug release

# ACKNOWLEDGEMENT

I am deeply indebted to express my sincerest appreciation to my esteemed mentor, the erudite Prof. Dr. Ömer ANDAÇ, whose guidance, profound insights, and enduring support have been instrumental in shaping the trajectory of this master's thesis. His deep wisdom and limitless understanding have gracefully illuminated my research path.

Furthermore, I am profoundly grateful to my cherished companions who were like a family for me during my sojourn away from my homeland and loved ones. Their true camaraderie and their presence provided solace and a profound sense of belonging amidst the shadows of estrangement.

Last, but certainly not least, I wish to convey my deepest gratitude to my beloved family, with a special mention of utmost appreciation to my revered mother and father. Their unfaltering encouragement, unwavering belief in my abilities, and tireless support have been the bedrock of my academic pursuits throughout the years. Their constant presence and faith in my potential have been the wellspring of my perseverance and the driving force propelling me forward in my studies.

Batool AL-MAFRACHI

# CONTENTS

# SYMBOLS AND ABBREVIATIONS

| | |
|---|---|
| 2G | : Second generation |
| DDS | : Drug delivery system |
| CS | : Chitosan |
| PVA | : Polyvinyl alcohol |
| PVP | : Polyvinylpyrrolidone |
| nHA | : Nano-hydroxyapatite |
| HAP | : Hydroxyapatite |
| TGA | : Thermogravimetric Analyses |
| DSC | : Differential Scanning Calorimetry |
| SEM | : Scanning Electron Microscopy |
| FTIR | : Fourier transform infrared spectroscopy |

# FIGURES LEGENDS

# TABLES LEGENDS

# 1. INTRODUCTION

## 1.1. Drug Release: A Historical Overview

Drug release has been an important subject in the field of drug delivery for many years. The advancement in materials design and engineering has produced new materials for the drug release application. This evolution also has added complexity and more functions to the drug delivery systems and devices. Drug release is the process by which drug solutes diffuse from their initial location within the polymeric matrix to the polymer's surface and subsequently into the surrounding release medium (Langer, 1990).

Prior to 1950, all medications were produced as capsules or pills without the ability to regulate the release kinetics, immediately releasing the loaded drug upon contact with water. After that in 1952, Kline and French Laboratories developed the first controlled release formulation capable of controlling drug release kinetics while achieving 12-hour effectiveness (P. Lee et al., 2010). The system, termed "Spansule technology," controlled the kinetics of the drug release at a specified period possible. Whenever the new controlled drug delivery system was first developed, numerous labels were used to characterize newer formulas with small changes from one another. Anyway, the term "sustained release" has become increasingly common than any others (Lafayette, 2016).

However, following several periods of developments in drug delivery methods, the little changes in functionality that various names imply are no longer necessary. The majority of the fundamental knowledge on drug release processes was gained from 1950 to 1980 this period is classified as the first generation of drug release development. During this time, four drug release mechanisms were discovered, which aided in the advancement of controlled release formulations (ion-exchange-controlled, osmosis-controlled, diffusion-controlled, and processes controlled by dissolution). Subsequent to that, various approaches for achieving prolonged drug release in the body have been developed; for example, numerous medications have been redesigned in Spansule systems by replacing wax coats with more reliable and consistent synthetic substances that can degrade progressively (Lafayette, 2016; W. Zhang et al., 2017). Diffusion-controlled and dissolution-controlled systems have been the most extensively employed methods. Although osmosis-based formulations were briefly popular, osmosis-based systems are much less common than those that utilize the other

two processes. Even though the ion-exchange technique is unique compared to others, it is ineffectual without the diffusion-controlled mechanism. However, a lot of oral once-daily formulas today rely on a diffusion- or dissolution-controlled mechanism (Yun et al., 2015).

The period after that which is termed the second generation has not been as effective as first-generation, as evidenced by the number of clinical items created (Park, 2016). One explanation for this is that second-generation technology handles more challenging formulations. It was considered at the time that maintaining a constant drug concentration is optimal; so, the studies aimed at creating drugs with a consistent rate of release (zero-order DDSs). For instance, biodegradable poly (lactic-co-glycolic acid, PLGA) injectable depot formulations are intended to provide peptide and protein medications for 30 days and more. First burst release, that frequently disperses 50% of the medication's total dose during the first day or two, is challenging for the majority of depot formulations to regulate (Ye et al., 2010).

After ten years of extensive research, it has been discovered that kinetics is not strictly required for a drug delivery system to categorize it as a sustained release since zero-order release is unable to keep the drug concentration constant on its own. Furthermore, the drug concentration doesn't need to stay at a steady level; the dosage effectiveness can still be maintained even if the concentration fluctuates between minimal toxic concentrations (MTC) and minimal effective concentration (MEC). Although it took nearly ten years for this evident truth to be discovered, this finding led to a more adaptable design for further drug delivery systems (Park, 2014). Smart polymers and hydrogels were created during this period. The unique trait that differentiates them from other materials is their sensitivity to changes in present parameters like pH, light, temperature, and electric field (P. Gupta et al., 2002). In addition to these developments, 2G was developed to distribute peptides and proteins over monthly time frames employing biodegradable microparticles (Brannon-Peppas, 1995), solid implants (Rosen et al., 1983), and implants that form a gel in situ (Hatefi & Amsden, 2002).

Last ten years has spent focusing on tumor-targeted drug delivery using nanoparticles. Numerous clinical trials have revealed that promising nanoparticle methods that depend on tiny animal models have failed (B. K. Lee et al., 2015; Park, 2013). The fundamental problem with 2G DDSs is that their physicochemical qualities

cannot be changed to get around biological barriers or change their negative effects on the human body. As a result, the 2G systems emphasize that simultaneously overcoming biological and physicochemical constraints is the key to success in the development of useful DDSs. Therefore, to get around physical, chemical, and biological limitations for novel delivery systems researchers should assemble and apply many disciplines (such as material science and engineering, physiology, biology, and computer science). We also need to understand the precise impact of employing each new material on the physicochemical and biological characteristics of the body, even though new materials always get a considerable interest in drug delivery research (W. Zhang et al., 2017). On the opposite side, the biological barriers depend on resolving problems with DDS dispersion in the body and improving its circulation throughout its half-life (Yun et al., 2015; W. Zhang et al., 2017).

The second generation of drug delivery methods' low effectiveness is primarily resulting from their incapacity to combat the physiological reactions following parenteral drug administration. However cleverly designed the present drug delivery systems may be, they are unable to meet the demands of the unpredictable and little-understood biological environment. To get through physicochemical and biological obstacles, the third generation of drug delivery technological advances ought to be far more sophisticated than the 2G methods. Comprehending and conquering biological hurdles besides physicochemical issues is an essential component of success., as seen by the summary of the 2G technologies above (Yun et al., 2015).

### 1.2. An Overview of Major Drug Release Mechanisms

There are several options for regulating medication release in an organism. Depending upon the application, the delivery steps may be finished concurrently or sequentially. It is essential to comprehend these procedures to develop and create controlled release systems. The releasing system also utilizes several chemical and biological methods. In essence, it is typical for a system to display more than one.

Based on the primary mechanism, controlled DDSs are categorized in terms of their mechanism of release. An overview of the different essential release mechanisms that are often present in drug delivery systems is provided in this section.

#### 1.2.1. Diffusion

Diffusion via the polymeric matrix acts as the main technique for controlling the release of drugs in diffusion-controlled drug delivery (Jamaledin et al., 2020). The

used polymeric matrix is not soluble in water. Polymers used for these systems contain chitin, polyethylene, polyurethane, or ethyl cellulose.

Diffusion DDs may also be categorized into reservoir and matrix-based systems. Systems based on reservoirs or matrixes can be separated into nonporous and porous modules (Jamaledin et al., 2020).

In reservoir type of system, three are water diffusion, drug dissolution, and drug diffusion. Scientists often presume that drug diffusion is the step that occurs most slowly. Additionally, it is believed that matrix material degradation is not considerable. accordingly, drug molecules are able to attain a zero-order release profile in reservoir systems if the depot's activity source is greater than necessary. In other words, if the initial drug loading is much higher than the solubility of the drug, a consistent drug release rate may be achieved regardless of the device's shape (Wang et al., 2020).

For the matrix-releasing method, the drug is spread across the monolithic noneroding matrix. As mentioned in the reservoir system, drug diffusion is the rate limiting stage. The release mechanism of this type of system is distinct because there isn't a barrier to control how quickly the interior core breaks off, like a membrane or microcapsule. Such a kind of system frequently has a high initial drug release afterward having a lower release rate as a function of time because it takes longer for the drug to diffuse to the surface as it goes deeper within. As a result, the vehicle's form significantly impacts how quickly drugs are released. By making up for the greater diffusion distance with larger surface areas, certain specialized forms, including hemispheres (Siegel, 2000) and cylinders (Jooybar et al., 2021) with appropriate coatings, can counteract the burst effect and offer near-zero-order release for long term therapy. Matrix systems come in a variety of forms. (Langer, 2007):

• Using a technique known as solution-diffusion, the medication is dispersed or dissolved in the matrix and diffuses outside of it.

• The substance diffuses through pores and channels in the matrix.

The porous matrix system is preferable for continuous medication release with high molecular weights, in contrast to the typical reservoir system, which is not able to achieve the extended release of large molecules (Wang et al., 2020).

### 1.2.2. Dissolution

Dissolution is the process of dissolving the molecules of a solute in a solvent. Drug molecules or ions are transferred from an active agent's solid phase to the surrounding media during the dissolving process generally water, in some cases polymer. When a solute is present in a solution to the extent of solubility under the circumstances of pressure and temperature, a solution is considered to be saturated. Supersaturated solutions are those that hold the solute inside the solution over the usual solubility level and can be created under specific conditions. These systems have polymeric components, such as natural gums, starch, poly (vinylpyrrolidone), poly (vinyl alcohol), as well as hydroxypropyl methylcellulose (Singh et al., 2019).

Utilizing the rate at which the drugs dissolve from the solid, it is possible to estimate the drug's rate of release from the system. When no chemical reaction occurs, the solubility is the higher with rapid dissolution rate (Santos, 2006).

The process of dissolution begins when the solvating environment around a solid drug particle is not fully saturated. Overall solvating medium, the solid's surface area, the thickness of the boundary layer, as well as the diffusion coefficient can all affect this process. The solid surface interacts with the dissolution medium when it is connected with it, which causes the molecules to solvate and separate from the solid. A number of solvated molecules (solute) rise in the medium, raising the solute concentration. As the solute concentration rises, the dissolution medium becomes saturated and the rate of dissolution decreases, enclosing the solid in a boundary layer. The solvent is renewed when the border layer is removed, accelerating the dissolution process.

These systems may be divided into matrix-based and reservoir-based systems. The drug molecules are contained inside a polymeric membrane in reservoir systems. The biomolecules are instantly and fully released into the environment when the membrane dissolves. The kinetics of drug release in this kind of system is determined by the thickness of the membrane and the dissolving kinetics of the polymeric formulation. A matrix-based approach evenly distributes the medication across the polymer matrix. As the matrix component disintegrates, the medication is liberated (Jamaledin et al., 2020).

### 1.2.3. Erosion

The polymers utilized in diffusion-controlled drug-release systems serve a relatively passive purpose. They operate as carriers and slow down the distribution of the active drug to the intended target. Some polymeric carriers have been developed to take a more active part in the delivery of drugs. When these polymers undergo chemical interactions, they erode, releasing the active ingredient. These systems are useful for implanted or injectable treatments since they do not need to be retrieved once the active drug has been fully released. The three biodegradable polymers that are most frequently utilized are poly (glycolic, poly (lactic-co-glycolic), and poly (lactic acid) (Marcos Luciano Bruschi, 2015; Singh et al., 2019).

They are classified into two categories: physical immobilization system and chemical immobilization system as seen Figure 1.1. In the first class, the polymeric net physically immobilizes the active agent, which is then released once the net has eroded. These systems are also referred to as biodegradable or erodible (Marcos Luciano Bruschi, 2015)

When the drug is chemically bonded to the polymeric matrix or is already a part of the design, the system is classified as a chemical immobilization (second group). An erodible system has clear benefits, particularly for pharmaceutical applications. After being administered, the system will disappear from the location, thus removal won't require any intrusive procedures. In erosion, products must, however, be harmless and resorbable or excretable (Marcos Luciano Bruschi, 2015).

The fundamental factor controlling the drug release from this type of system is the kinetic decomposition of the relevant link, that varies between systems. Surface erosion and bulk erosion are two behavioral boundaries that need to be taken into account in erodible systems. Either a slow water invasion or quick hydrolysis causes the system's surface to erode. When a polymer is hydrophobic, the interior of the polymeric system is shielded from water so that its chemical linkages that are sensitive to hydrolysis are not exposed. Therefore, only at the surface or very near it does hydrolysis with the concomitant release of the active substance take place. With time, surface erosion causes the system's dimensions to shrink.

It is nearly impossible to produce pure surface erosion, and before erosion has a place, a medication may diffuse out of a matrix. The medication itself may attract water, and osmotic tensions in the polymer (due to small chain fractures) may cause

breakage and unequal penetration. The primary mechanism of polymeric erosion is bond hydrolysis, which can be base or acid catalyzed depending on the number of donors and acceptors of protons in the area (Marcos Luciano Bruschi, 2015).

Similar to systems controlled by diffusion an erodible system with the active ingredient physically inserted can be created (reservoir or monolithic systems). Nevertheless, if the surrounding media like water infiltrates the system faster than hydrolysis can, water will be present throughout the material, chain scission processes start everywhere and bulk erosion happens.

Initial scissions may give chains enough mobility to move forming crystallites, that are less sensitive to hydrolysis. It is initially characterized by relatively sluggish hydrolysis. Once a specific grade of hydrolysis has taken place, the process could quicken. By diffusion and/or osmosis, the creation of short chains may result in a general loss of polymer and a rise in water concentration. Additionally, erosion will be autocatalytic if chain scission causes the creation of acidic end groups and the scission process is acid-catalyzed (Marcos Luciano Bruschi, 2015).

Bulk erosion normally goes through the three stages. The drug first leaves the system through pores that are attached to the surface of the body or from the surface itself. The second step is known as the latent stage, during which the residual active agent is confined and a small amount of polymer breakdown occurs. The confined active ingredient is swiftly released in the final stage when the polymer breaks down. Because auto-catalytic erosion products build up inside the system, it degrades quickly there while the surface erodes more slowly as a result of their leaching. Matrix thickness can affect how soon it degrades; thicker matrices might degrade more quickly when this is the case (Siegel & Rathbone, 2012).

The most prevalent erodible systems are based on poly (lactic acid). Systems based on poly (ortho esters), polyanhydrides, polyphosphates, and polyphosphazene have also been used or researched (Wilson & Crowley, 2011).

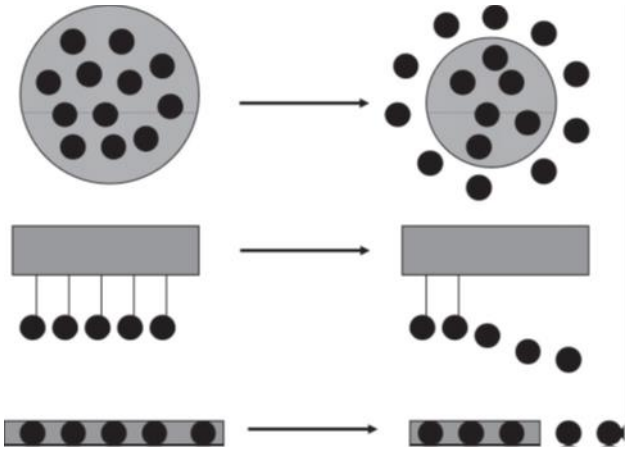

Figure 1.1. Erosion system: (a) physical immobilization. (b) chemical immobilization (Marcos Luciano Bruschi, 2015)

### 1.2.4. Osmosis

Osmosis is the method used to dilute a solution made up of a solute and a solvent by passing the solvent across a semipermeable membrane. The solvent will tend to flow through the semipermeable membrane from the less concentrated solution to the more concentrated solution when two solutions of different concentrations are separated by it and the membrane is permeable to the smaller solvent molecules but not to the large solute molecules. Equalizing the concentrations of the impermeable solutes on both sides of the membrane is the goal. The solvent when it comes to biological organisms is water. The movement of molecules, including water, through biological membranes, is crucial to a number of activities in living things (Siegel & Rathbone, 2012).

The nature of water transport for active chemicals, however, may not be as straightforward as this idea suggests. The chemical potential, which regulates both the flux of water through the membrane and the gradient of water concentration, is dependent on the concentration of solutes, or osmolytes, and the thermodynamic compatibility of water with these osmolytes. When the osmolytes are small molecules (like salts), the concentration of the osmolyte primarily determines the osmotic pressure but when the osmolytes are polymers, the osmotic pressure is affected by both the concentration of the polymer and how well it interacts with water (Siegel & Rathbone, 2012).

The rate of solvent through the membrane transportation increases with the magnitude of the chemical potential gradient, given the connection between chemical potential and osmotic pressure as well as the membrane's hydration has caused the

water molecules to be in motion and in touch with one another (Siegel & Rathbone, 2012).

Drug-release systems based on diffusion and erosion are typically easier to design and more efficient in terms of volume than osmotic systems. Nevertheless, osmotic systems frequently provide superior zero-order delivery, delivering a greater portion of the drug loading at a constant rate. (Mathiowitz, 1999).

### 1.2.5. Swelling

Many materials exhibit the property of swelling when it is in contact with water. This is a result of their hydrophilic property and how water and its molecules interact. The primary components used to create controlled drug release systems are polymers, and these materials have polymer chains that can arrange into three dimensions. Water causes a polymer network to expand and generate chemical or physical connections. The swelling procedure is extremely comparable to osmosis. Water ingress into the polymer matrix is a rapid process, while the dissolution of the polymer in water proceeds comparatively slowly, attributed to the necessary separation of the polymer chains (Siegel & Rathbone, 2012).This increase in volume and the resulting creation of larger pores between the polymeric chains can be exploited to regulate how quickly active agents are released from polymeric systems. The morphology of the matrix can be used to macroscopically observe the significance of the swelling (in reservoir systems).

A polymeric matrix's ability to absorb water results in an increase in thickness and volume during the initial phase of drug release. This increase in thickness is countered by the subsequent disentanglement of polymeric chains and the dissolving of the drug utilized, which results in a decrease in the matrix's volume. When the entire polymer is inflated, the matrix finally dissolves as seen in Figure 1.2.a. A "swellable-soluble matrix" is a better name for this type of system (Colombo, 1993).

Swelling frequently occurs before polymer degradation. Nevertheless, there are instances where the material's swelling is constrained, and the matrix does not undergo dissolution, Figure 1.2.b. The occurrence of this phenomenon can be attributed to factors such as insufficient compatibility between the polymer and water, polymer chain length exceeding a critical threshold, or the introduction of cross-linking agents leading to the formation of a polymer structure (Siegel & Rathbone, 2012).

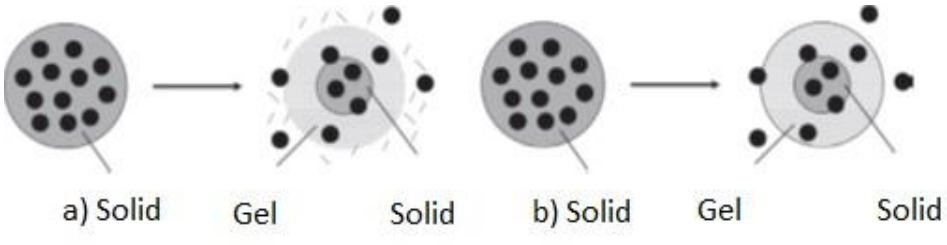


Figure 1.2. The process of swelling that occurs during the time period between t0 and tt : (a) unlimited (b) limited (Marcos Luciano Bruschi, 2015)

The process of water absorption and swelling is typically governed by the interplay of various forces such as osmotic, electrostatic, and entropy-driven dissolution forces that affect the polymer. The elastic properties of the hydrogel are designed to regulate the entropy associated with the dissolution process (Omidian & Park, 2008). The extent of swelling is determined by the polymer's hydrophilicity as well as the degree and density of cross-linking among its chains. Hence, hydrophobic polymers exhibit a weak affinity towards water and undergo negligible swelling (Siegel & Rathbone, 2012).

As a result, the drug release is going to be managed by the rate of swelling. The swelling agents can be classified into chemical and physical categories. The polymers in the first category have all of their chains connected to one another by covalent bonds. A cross-linker is used to combine the polymeric chains during the manufacture of chemical polymeric material. A physical polymeric is formed when the hydrophilic precursor is handled physically; therefore, functional groups capable of reacting with ions or aldehydes should be contained in polymers (Colombo, 1993).

When the system comes into contact with water, the rigid polymer layer on its surface relaxes and transforms into a more water-friendly configuration, leading to the swelling of the system. This process facilitates the penetration of water into the material, often leading to the formation of a moving front that delineates a swollen outer layer from a dry inner core, Figure 1.3.

The control of the swelling process is contingent upon the polymer network's cross-link, ionic content, and hydrophilic content. The precise tailoring of swelling kinetics, achievable through means such as cross-link density modulation, offers an avenue for the design of advanced controlled release systems (Omidian & Park, 2008).

The polymeric chain relaxation often results in a transition from a glassy to a rubbery state. The swelling behavior and release kinetics can be modulated by a range of factors, including additives, the active ingredient, choice of polymer, pH, and temperature. By alternately manipulating these parameters, by inducing reversible swelling and shrinking of hydrogels, it becomes possible to achieve a pattern of drug release that can be turned on or off (Siegel & Rathbone, 2012).

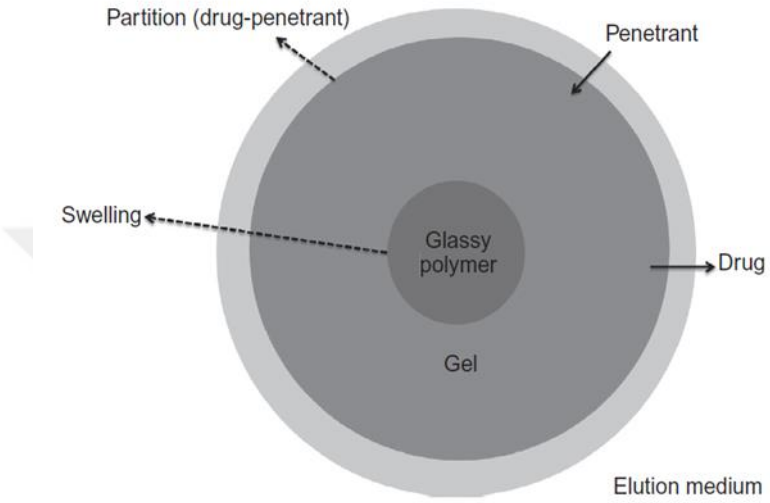


Figure 1.3. A diagrammatic illustration of the phenomenon that takes place in release systems controlled by swelling (Marcos Luciano Bruschi, 2015).

### 1.2.6. Pendant-Chain-/Prodrug-Based Mechanism

One approach for releasing drugs involves chemical alterations to create drug-carrier conjugates, at which the drug is released based on enzymatic or hydrolytic fragmentation. Instead of the system itself, external factors like the pH level and enzymes have a greater impact on the release kinetics (Ashton et al., 2000). The type of appliance material and coupling technique can also influence the release rate. For example, incorporating carboxylic groups in acidic antibiotics enables them to bind to phosphate groups or form a chelate with calcium ions that can be released at a slower, more gradual rate (Stigter et al., 2004). A spacer group can be used to further regulate the release rate for long-term drug distribution by acting as a linker between the medication and the carrier material (Battig et al., 2012; Vulic & Shoichet, 2012).

For long-term applications in polymeric systems, using a non-degrading polymer basis to attach drugs is preferable, however, this poses possible issues. For instance, the device may need to be physically removed if a long-term accumulation of materials results in local tissue responses. This kind of device can be used to supply proteins

over an extended period of time while conserving their structures and functions and minimizing burst release. Obstacles exist because of the considerable variation in environmental factors among people, illness states, and homeostasis because these factors may make it challenging to anticipate the underlying dynamics of controlled release. For instance, particular prodrugs for the colon are prone to a variety Regarding individual variations in the microflora's composition (Jung & Kim, 2010).

### 1.2.7. Stimulus-Activated or Modulated Mechanisms

The final class of drug release systems utilizes external stimulation to start releasing mechanism (Priya James et al., 2014). When exposed to external stimuli, polymeric systems undergo physical or chemical changes that lead to the release of drugs. The polymer's composition and structure, the kind and the strength of the outside stimulation, and the ambient circumstances all impact the kinetics of drug release in these mechanisms. For instance, the pH of microneedles used to deliver insulin is frequently used as a trigger for drug release, and both pH-sensing (pH-responsive/polymer) and glucose-sensing (often glucose oxidase) components are present in these delivery vehicles. The enzyme glucose oxidase transformed the glucose that the microneedles were exposed to into gluconic acid. The pH of the surrounding environment was subsequently lowered as a result. The pH drop changed the pH-responsive substance's characteristics and further triggered the release of insulin (Xu et al., 2018).

## 1.3. Hydrogels and Biopolymers for Drug Release Applications

Hydrogels are a special class of drug release system (X. Li et al., 2018; Niu et al., 2019) that have been used in numerous medical fields, including pain relief, wound healing, immunology, cancer, and cardiology (J. Li & Mooney, 2016). Hydrogels are a polymeric network that is hydrophilic and three-dimensional. that has a high capacity for absorbing water or other biological fluids. In actuality, water demonstrates thermodynamic compatibility. Functional groups within hydrogels contribute to their hydration and subsequent water absorption capacity (such as $SO_3H$, CONH, $CONH_2$, COOH, etc.). Van der Waals and ionic bonds also allow them to withstand volume fluctuation, exhibit consistent strength, and resist dissolution (Nho & Park, 2002).

Hydrogels are valuable in a variety of biological fields (Hafeez et al., 2018) because of their biocompatibility (George et al., 2019), biodegradability (Cong et al., 2018), softness, super absorbancy (Rizwan et al., 2017), and mechanical strength

(Maitra & Shukla, 2014). The swelling ratio of hydrogels is influenced by the presence of hydrophilic groups, the density of cross-linking, and the nature of the swelling media (Gierszewska-Drużyńska & Ostrowska-Czubenko, 2011).

Hydrogels produced from polymers using noncovalent methods are advantageous for drug release systems since they don't require any chemical reactions that could affect drug release. These hydrogels are created through hydrogen bonding or hydrophobic interactions (Martin et al., 2002).

The most important factors to consider when choosing the right polymer for these applications are its molecular weight, solubility, wettability, structure, degradation mechanisms, and fabricability (Anju et al., 2020).

Due to the intricacy of the physicochemical requirements listed above, considering the development of biomaterials, it is not possible to designate any polymeric system as an ideal choice. The production of polymeric systems with controllable characteristics for the design objective is therefore made possible by mixing polymers. Meanwhile, the development of biopolymer and nanoparticle combinations remains an exciting area of research (Bhattarai et al., 2018).

Blends of natural and synthetic polymers create cutting-edge materials with many applications. To improve the qualities of natural polymers, synthetic polymers are combined with them (Bahrami et al., 2003). The idea of blending polymers was inspired by the realization that new molecules are not always enough to fulfill the requirements of sophisticated materials and that blending is a realistic option to achieve the needed qualities instead of developing new materials (Jaganathan, Mani, et al., 2019; Jaganathan, Prasath Mani, et al., 2019) So, blending means the mixing of various polymers to attain desired characteristics (Giang Phan et al., 2019; Liu et al., 2005) .

### 1.3.1. Chitosan

Chitosan is a natural cationic polymer obtained from the deacetylation of chitin (Johns & Rao, 2008). It counts as the second-most prevalent polymer in nature. Enzymatic and chemical processes are used to create chitosan oligosaccharides from chitosan. Its molecular weight is very less (3900 Da). Astonishing characteristics of chitosan oligosaccharide include its water solubility, nontoxicity, anti-inflammatory effects, and antioxidant capacity (Bockuviene & Sereikaite, 2019) Numerous research

studies on chitosan-based formulations have been reported for various biomedical applications (Kucharska et al., 2015; Tsao et al., 2014).

The chemical Chitosan's structure is comparable to cellulose's, with the exception that one of the hydroxyls (-OH) groups in the repeating unit is replaced by an amino group ($-NH_2$). Chitosan is a polysaccharide with a linear structure that consists of D-glucosamine (deacetylated unit) and N-acetyl-D-glucosamine (acetylated unit) arranged in a random distribution. The degree of deacetylation (DDA) determines the ratio of these two units, with higher DDA indicating more glucosamine units and fewer acetylglucosamine units. The chemical formula for chitosan can be represented as $(C_6H_{11}NO_4)x$, where x represents the number of repeating units (Rinaudo, 2006).

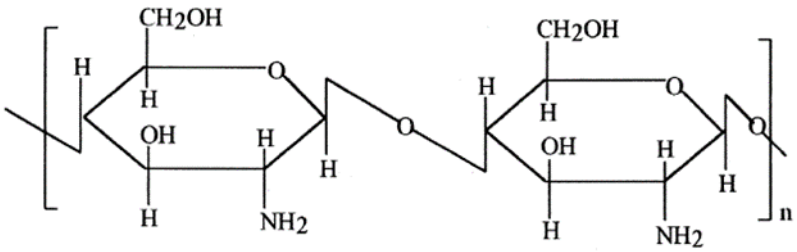


Figure 1.4.Chemical structure of chitosan (Ravi Kumar, 2000)

The hydrogels based on chitosan have been widely studied for drug delivery applications (Giri et al., 2012), The cationic properties of chitosan arise from the existence of an amine group that allows them to adhere to negatively charged biological surfaces like mucosal glycoproteins (He et al., 1998; Lehr et al., 1992). This makes chitosan a suitable bioadhesive material, which prolongs the residence time of the drug loaded system and provides localized drug delivery (Peppas & Sahlin, 1996). Additionally, chitosan plays a crucial role in mediating the paracellular transportation of drugs, leading to a substantial impact on the efficiency of drug delivery systems (De Campos et al., 2001). Chitosan has been employed as a drug carrier because it is biocompatible, biodegradable, and has a readily modifiable structure.

Chitosan has excellent blending properties with synthetic polymers (Grande et al., 2018). Chitosan and hydrophilic polymers can be combined or blended to change their functional properties (Elashmawi & Elsayed, 2020). Chitosan is capable to combined with synthetic or natural polymers using various approaches to achieve specific properties. These methods include chemical crosslinking of chitosan,

changing the structure of chitosan chains to create a crosslinking agent, facilitating hydrophobic interactions, enabling electrostatic interactions, and promoting hydrogen bonding (Sacco et al., 2016; Yoo et al., 2016). Chitosan hydrogels can also be formed through the interaction of the amine groups between polymer chains via hydrogen bonding (Baghaie et al., 2017; Mahdavinia et al., 2018).

The primary benefit of utilizing the physical cross-linking method is the absence of crosslinking agents, which can reduce biocompatibility. Moreover, physically crosslinked hydrogels possess the ability to self-heal. These hydrogels can be formed via interactions with small negatively charged molecules, polyanions, the formation of hydrogen bonds, or hydrophobic interactions. One method employed for the production of physical hydrogels based on chitosan is through association using electrostatic interactions. To crosslink chitosan, it is common to employ anions such as phosphate-bearing molecules, polyacrylic acid, sodium alginate, heparin, and polyglutamic acid. These anionic compounds facilitate the crosslinking process and contribute to the formation of hydrogels (Mohamed et al., 2017).

The incorporation of chitosan with other polymers offers the advantage of creating a hybrid material that possesses distinctive properties. For example, physically crosslinked chitosan-based hydrogels are responsive to external stimuli like pH and temperature due to their noncovalent nature (Sacco et al., 2016).

### 1.3.2. Poly (vinyl alcohol)

Poly (vinyl alcohol) (PVA) is a biodegradable polymer that is hydrophilic and Each monomer polymerized from vinyl acetate contains a singular hydroxyl group. It should be noted that the hydrolysis of the polyvinyl acetate is dependent on the molecular weight of the polymer, as a consequence, poly (vinyl alcohol) (PVA) is formed, which is a blend of poly (vinyl alcohol) and poly (vinyl acetate). In high-grades of PVA, the proportion of poly (vinyl alcohol) can reach 99% (Kenawy et al., 2010).

So, PVA is a synthetic polymer with the chemical formula $(C_2H_4O)_n$ having a molecular weight that can vary depending on the length of the initial vinyl acetate polymer and the degree of hydrolysis, typically ranging from 20,000 to 400,000 g/mol. PVA is commonly categorized into two grades: partially hydrolyzed and fully hydrolyzed, depending on the extent of the hydrolysis process. The chemical structures of PVA can be observed below in Figure 1.5 (Gao et al., 2010).

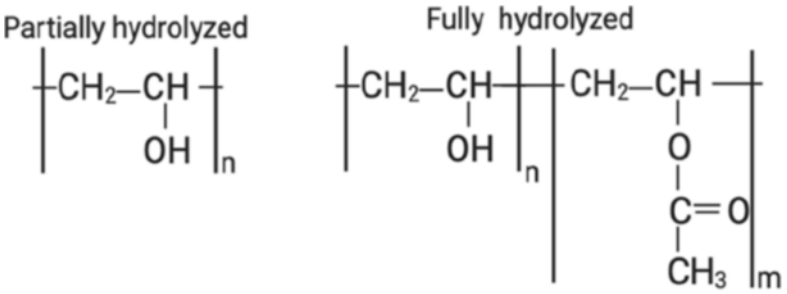


Figure 1.5.The partially and fully hydrolyzed structural formulas of PVA (Gao et al., 2010)

In general, PVA typically possesses water solubility while exhibiting slight solubility in ethanol and insolubility in organic solvents. It is known for its absence of taste and odor. The properties of PVA, including (pH, viscosity, drying behavior, melting point, refractive index, and residue on ignition), depend on both its molecular weight and the extent of hydrolysis. For instance, PVA with a moderate hydrolysis degree (87-89%) shows increased water solubility, enhanced flexibility, and improved adhesion to hydrophobic surfaces. On the other hand, highly hydrolyzed PVA (91-99%) demonstrates enhanced stability in the presence of organic solvents, elevated tensile strength, and superior adhesion to hydrophilic surfaces (Rowe et al., 2013).

The presence of hydroxyl groups in PVA leads to the formation of inter- as well intramolecular hydrogen bonds. The density and arrangement of these hydroxyl groups determine the viscoelastic and structural properties of the polymer (Gao et al., 2010). The hydrogen bonding also contributes to the occurrence of gelation and phase separation, making the solution characteristic time-dependent. The viscoelastic and rheological characteristics of PVA solutions are influenced by the efficiency of the physical interactions, polymer chain length, and molecular alignment (Gao et al., 2010; Song & Kim, 2004).

The mechanical characteristics, film-forming capability, lack of toxicity, water solubility, hydrophilicity, favorable compatibility, and biodegradability in fluids and human tissues have made PVA one of the most commonly used polymers in the biomedical field (Hassan & Peppas, 2000; Luo et al., 2018; Rolim et al., 2019). Additionally, PVA exhibits three essential properties that are crucial for it to serve as an effective delivery system: strong surface stabilization, chelation capabilities, and low protein adsorption properties. These characteristics contribute to minimal cell adhesion when compared to other hydrogels (Baker et al., 2012; Fatema et al., 2018; Kadhim et al., 2016).

Despite having such advantageous qualities, PVA has certain disadvantages, including a high capacity for swelling and solubility in water. The mechanical properties of polymeric membranes based on polyvinyl alcohol are quite poor as a result of these limitations (Ollier et al., 2012).

Extensive researches have demonstrated the effectiveness of PVA in the formulation of hydrogels. PVA hydrogels can be cross-linked using a variety of methods including chemical and physical methodologies (Rivera-Hernández et al., 2021)

In the last years, there has been a growing interest in combining PVA and chitosan. Blended films of chitosan and Polyvinyl alcohol (PVA) are utilized as medical tools and for drug delivery purposes (Srinivasa et al., 2003).

Combining PVA and chitosan can result in the formation of a hydrogel with a three-dimensional network due to the physical interactions between the two polymers. This is a significant advantage because it eliminates the need for crosslinking agents. By forming such a network, the mechanical properties of the polymer matrix are improved, ultimately resulting in a more robust drug delivery system (Sánchez-Aguinagalde et al., 2021).

### 1.3.3. Polyvinylpyrrolidone

Polyvinylpyrrolidone (PVP) is a polymer that has good solubility in water and is produced by polymerizing the monomer N-vinylpyrrolidone. It exhibits non-reactivity, non-toxicity, temperature resistance, pH stability, biocompatibility, and biodegradability. It can effectively encapsulate and accommodate a wide range of drugs, both hydrophilic and lipophilic in nature. These properties make PVP an adaptable excipient in formulating various conventional and innovative controlled delivery systems (Kurakula & Rao, 2020). PVP not only functions as a hydrophilic polymer but also exhibits remarkable solubility in solvents with various polarities. Moreover, it possesses strong binding properties and can stabilize suspensions and emulsions ( Folttmann & Anisul, 2008).

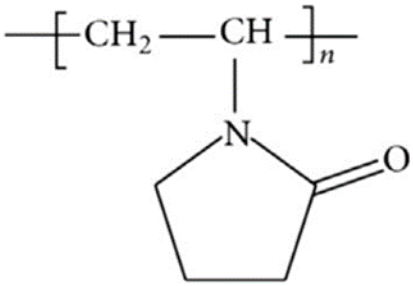


Figure 1.6.The chemical structure of PVP

PVP has demonstrated versatility in the pharmaceutical and biomedical fields for the development of various drug delivery systems, including oral, topical, transdermal, and ocular administration. Additionally, PVP has been utilized in gene delivery (Saxena et al., 2006; Sheu et al., 2005; Song et al., 2015; Zhang et al., 2009; Zheng et al., 2015) , coupled with metal particles for regenerative medicine (De Lima et al., 2018; Hecold et al., 2017; Hu et al., 2018), and targeted delivery (Ramalingam et al., 2018; Rose et al., 2013). Thus, PVP is a highly versatile polymer with various applications. It enables the controlled release of drugs, enhances the bioavailability of drugs that have low water solubility, shields the active compound from external factors (such as pH, temperature, and oxygen), and masks unpleasant odors and flavors (Ajji et al., 2020; Fogaça & Catalani, 2012; Mishra et al., 2008; Raneque et al., 2013; Risbud et al., 2000) Some research papers have proposed PVP-based hydrogels and oral tablets (Janugade et al.,2009; Karavas et al., 2006; Raneque et al., 2013; Wlodarski et al., 2016). PVP also has an exceptional ability to form films, as demonstrated in several studies (Diaz del Consuelo et al., 2007; R. Gupta & Mukherjee, 2003; Mohabe et al., n.d.; Perioli et al., 2004; Sadashivaiah et al., n.d.).

When combing PVP with natural polymers like chitosan, affords hydrogels favorable properties for controlled drug delivery (Rasool et al., 2019). A key factor in enhancing the connection between chitosan and PVP and creating the final hydrogel's qualities is the development of the hydrogen bond between the pyrrolidine rings of PVP and the hydroxyl and amino groups of chitosan. Results by Khoo et al. show that, when PVP is used in place of a chitosan hydrogel, this interaction improves the final hydrogel's mechanical, physical, and thermal properties (Sizílio et al., 2018).

### 1.3.4. Nano hydroxyapatite

Nano hydroxyapatite (nHA) is a type of hydroxyapatite with a nanoscale particle size, typically ranging from 20 to 100 nm. It has the same chemical structure as

hydroxyapatite found in human bone and teeth. The chemical formula for hydroxyapatite is $Ca_{10}(PO_4)_6(OH)_2$, where calcium ions ($Ca^{2+}$) and phosphate ions ($PO_4^{3-}$) form a hexagonal hydroxylapatite crystal structure. In nHA, the particle size is reduced to the nanoscale, which increases its surface area and allows for improved bioactivity and biocompatibility. The surface of nHA is typically coated with hydroxyl (-OH) groups, which provide a reactive surface for chemical interactions. These hydroxyl groups can form hydrogen bonds with other molecules, such as proteins or polymers, and facilitate their binding to the nHA surface (Dorozhkin, 2009).

In general, hydroxyapatite (HAP) is a type of biocompatible and bioactive ceramic that possesses the capability to establish direct bonds with living tissues, promoting integration with biological systems (Fathi et al., 2008; Rouahi et al., 2006). While there is some controversy regarding the safety of using inorganic nanoparticles, HAP is considered to be significantly more biodegradable and biocompatible than other types of nanoparticles (Yang et al., 2013). Compared to polymers, hydroxyapatite is pH-dependent, and it demonstrates a higher level of biocompatibility (Kester et al., 2008). Moreover, it demonstrates superior stability compared to liposomes and micelles, which tend to disperse at certain concentrations (Uskoković & Uskoković, 2011). Additionally, HAP is more soluble and has less toxicity than other materials such as $SiO_2$, $TiO_2$, carbon nanotubes, quantum dots, and magnetic particles (Contreras-Torres et al., 2017; Guerrero-Beltrán et al., 2017; Ornelas-Soto et al., 2017; Uskoković & Uskoković, 2011). Due to its crucial role in clinical applications and tissue engineering, this material has garnered significant attention and has been widely studied in the field of biomaterials science (Eslami et al., 2009). HAP's limited solubility under physiological pH conditions provides a valuable advantage, as it can be employed as a carrier for targeted drug delivery through surgical placement and injection (Matsumoto et al., 2004; Uskokovič & Desai, 2013). In addition, HAP nanoparticles possess osteoconductive, non-inflammatory, and nonimmunogenic features, making them an essential component of biomaterial design (Elbasuney, 2020; Khalid & Chaudhry, 2020; Sebastiammal et al., 2020).

Nanostructured bio-ceramics have been developed through nanotechnology, with HAP nanoparticles displaying excellent biocompatibility and biodegradability due to their size (with at least one dimension of 100 nm) (Dasgupta et al., 2009). Surface modifications can also be made to allow for hydrophobic interactions, charge

density, and pi-electron density, and the nanoparticle design can significantly impact interactions with the biological environment due to the large surface-to-volume ratio (Bai et al., 2017). HAP nanoparticles are well-suited as a biomaterial in the bone system due to their similarity in structure to bone minerals, which consist of small HAP crystals at the nanoscale, leading to more efficient osteoblast adhesion and proliferation (Fathi et al., 2008).

Over the years, extensive research efforts have been directed toward investigating the potential of HA in the context of bone tissue and related diseases. Additionally, the utilization of HA nanoparticles in drug delivery systems has demonstrated its remarkable affinity for both hydrophobic and hydrophilic drugs, as well as nucleic acids and proteins (Ginebra et al., 2012; Lee et al., 2014; Munir et al., 2018; Watanabe et al., 2013).

Drug delivery applications have made use of HAP nanoparticles in their pure form, as well as in combination with polymers, to achieve effective delivery of drugs, and there is a growing interest in the relationship between their physicochemical properties and biological applications. Biorelevant characteristics, including morphology, crystalline phase, size, shape, and functional groups play a crucial role in determining the nanoparticles' surface reactivity and biocompatibility (Galindo et al., 2019). The combination of hydroxyapatite with chitosan leads to an organic–inorganic composite material with improved biocompatibility and antimicrobial properties (Boudemagh et al., 2019; Pighinelli & Kucharska, 2013).

## 1.4. Related Studies and Research Objectives

### 1.4.1. Related Studies

In recent years, the development of hydrogels as drug-release systems has gained significant attention. Chitosan, polyvinyl alcohol (PVA), and polyvinylpyrrolidone (PVP) are commonly used hydrogel-forming polymers due to their unique properties mentioned earlier. Additionally, incorporating nanoparticles, such as nanohydroxyapatite (nHA), into these hydrogels can enhance their properties and make them suitable for biomedical applications. This review will provide an overview of the recent studies on synthesizing and characterizing different hydrogels based on these polymers and using nHA for drug release applications.

In the field of synthesis and characterization of chitosan, Iqbal et al. (2020) conducted a study to investigate the synthesis and characterization of ternary blends

hydrogel-film of chitosan, guar gum, and polyvinyl alcohol (PVA) formed by solution casting method. The study aimed to understand the effect of the material's percentage on the hydrogel. The results showed that the swelling properties of the fabricated membrane were found to be dependent on the concentrations of chitosan and guar gum. The membrane composed of 60% chitosan, 20% guar gum, and 20% PVA exhibited the highest swelling ratio, indicating the hydrophilic character of the membranes. Moreover, the ternary blends of chitosan, guar gum, and PVA have shown promise in the field of controlled drug delivery.

Eskitoros-Togay et al. (2020) performed a study in which nanosized hydroxyapatite (nHA) was added to a poly (ε-caprolactone)/poly(ethylene oxide) (PCL/PEO) blend matrix with or without curcumin. Electrospinning was used to fabricate composite fibrous material systems. The resulting material systems were analyzed for their morphological and physicochemical properties and their in vitro curcumin release behavior. The study found that there was no linear relationship between the release behavior of curcumin and the amount of n-HA incorporated in the polymer matrix. This suggests that adjusting the composition of n-HA could be a way to enhance the anticancer activity of curcumin by controlling its release profile.

In a prior study, Mahato et al. (2020) developed a new hydrogel film by crosslinking a composite of polyvinyl alcohol and chitosan oligosaccharide using glutaraldehyde via a solution casting method. The hydrogel film was evaluated for its drug delivery potential by conducting in vitro drug release study of Lomefloxacin. The results suggested that the hydrogel film has the potential to be utilized as a drug carrier for controlled release applications.

In a separate investigation by (Ghauri et al., 2021), a drug delivery system was developed using ternary hydrogel films as carriers. Hydrogel films were developed through the solution casting method, utilizing a polyelectrolyte complex of chitosan, guar gum, and polyvinyl pyrrolidone, cross-linked with sodium tripolyphosphate. The study aimed to assess the interplay between polymeric chains, surface morphology, thermal stability, swelling behavior, and drug release kinetics of the hydrogel films. The findings highlighted the integration of functional groups and interconnections within the blend components. The swelling capacity of the hydrogels decreased with higher cross-linker concentrations and exhibited pH-dependent behavior, with increased swelling under acidic conditions and reduced swelling under neutral and

basic pH levels. The hydrogel films demonstrated thermal stability over a wide temperature range, and the drug release analysis indicated their suitability for controlled drug delivery applications.

In a recent study by Iqbal et al. (2021), a hydrogel composed of chitosan, guar gum, and polyvinyl alcohol was synthesized through the solution-casting method for the sustained release of antibacterial drugs such as amoxicillin and doxycycline hyclate. The study confirmed successful surface morphology, blend formation, crystalline nature of the polymer, and effective bonding among the ingredients. The hydrophilic nature of the membranes was demonstrated through a swelling test, making them suitable for drug release applications. Promising antimicrobial activity was observed against selected bacteria and cytotoxic investigations showed their potential in various biomedical applications.

### 1.4.2. Research Objectives

The aim of the study was to synthesize and characterize a novel polymeric film. It is aimed to achieve the following specific goals:

- Synthesis of a novel hydrogel film from natural polymer and synthetic polymer combined with nanoceramic material. Chitosan, PVA, PVP, and nHA have been chosen for this purpose due to their unique properties. The hydrogel is physically cross-linked to avoid the reduced biocompatibility.
- Study the effect of nHA on the characterizations of the hydrogel and the drug release profile. This was an important consideration, due to a scarcity of scientific literature or a limited number of research studies investigating the effect of nHA on hydrogels for drug release application.
- To explore the mechanical and physical properties of the films created in this project.

# 2. EXPERIMENTAL

## 2.1. Materials

The medium molecular weight of chitosan, which had undergone 75-85% deacetylation, was acquired from Sigma-Aldrich Corporation located in the US.

Polyvinyl alcohol (PVA), which had a molecular weight of 13,000-23,000 and a degree of hydrolysis of 87-89%, was obtained from Sigma-Aldrich Corporation located in the US.

Polyvinylpyrrolidone with an average molecular weight of 5500 was obtained from Sigma-Aldrich Corporation located in the United States.

Nano-hydroxyapatite with a minimum purity of 99.95%. It has a particle size of 50 nm and is purchased from Nanokar, Turkey.

Acetic acid with a molecular weight of 60.05 g/mol. Purchased from Honeywell, Germany has a high level of purity, with a minimum purity of 99.8%.

Phosphate buffer saline (PBS) tablet purchased from Sigma-Aldrich Co., USA. This tablet can be dissolved in 200 ml of deionized water, resulting in a solution with a pH of 7.4 and containing 0.01 M phosphate buffer, 0.0027 M potassium chloride, and 0.137 M sodium chloride.

Ethanol with a minimum purity of 99.8% and molecular weight ($M_w$) of 46 g/mol was sourced from Honeywell, Germany.

## 2.2. Methods

### 2.2.1. Synthesis of Hydrogel Films

To prepare the hydrogel, chitosan was dissolved in a 1% acetic acid solution at a concentration of 1.75 g and stirred overnight until complete dissolution. Vacuum-assisted filtration was used to remove impurities from the chitosan solution, Figure 2.1. This process involved driving the solution through a filter membrane under negative pressure using a vacuum, trapping the impurities while allowing the purified chitosan solution to pass through.

Figure 2.1.Vacuum-assisted filtration

The preparation of 1% poly (vinyl alcohol) and 2% polyvinylpyrrolidone solutions in deionized water was achieved by dissolving the respective amounts of the polymers in water at 80 °C for an hour. The resulting solutions are depicted in Figure 2.3.


Figure 2.2. Raw materials

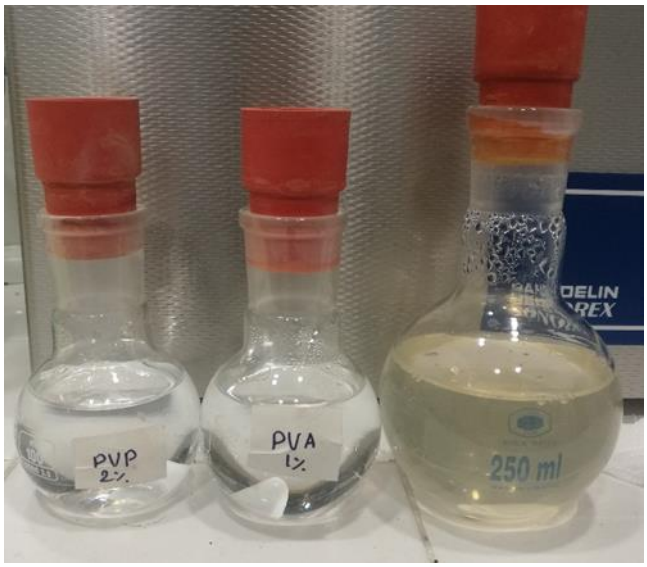


Figure 2.3. Solution of CS, PVA, and PVP

To synthesize the hydrogel, 40 mL of the chitosan solution was mixed with 20 mL of the poly (vinyl alcohol) solution for one hour, followed by the addition of 10 mL of polyvinylpyrrolidone to the mixture. This solution was stirred for an additional hour at 65°C. Next, nanohydroxyapatite (nHA) was added to the solution in varying concentrations (0, 10, 20, 30, and 40 mg) as a suspended solution and stirred for 3 hours at 65°C to produce different hydrogels and examine the impact of nHA on the properties of the films, Figure 2.4. The hydrogel solutions containing different nHA concentrations are presented in Figure 2.5.

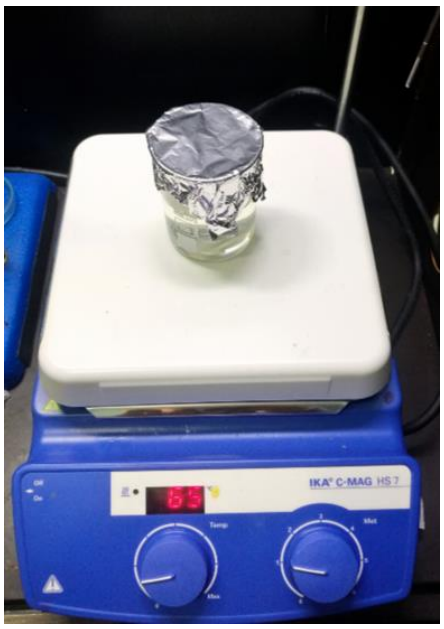


Figure 2.4. Mixing the final solution


Figure 2.5. CS/PVA/PVP solution with different % of nHA

The films were created by using the solution casting method, in which the hydrogel solution was poured into a Petri dish and dried at 50°C which is shown in Figures 2.6 and 2.7.

Figure 2.6. Solution casting

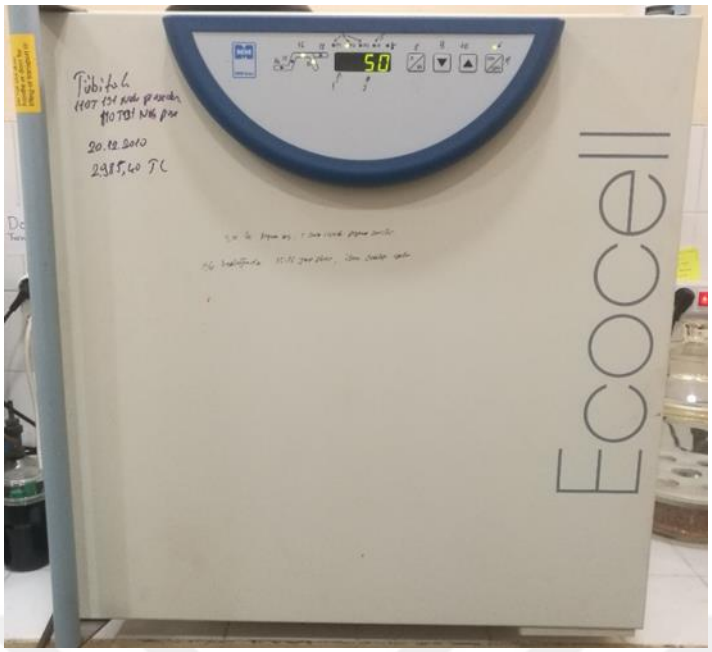


Figure 2.7. Fern used for the hydrogel drying

The resulting films, as shown in Figure 2.8, possess good transparency.

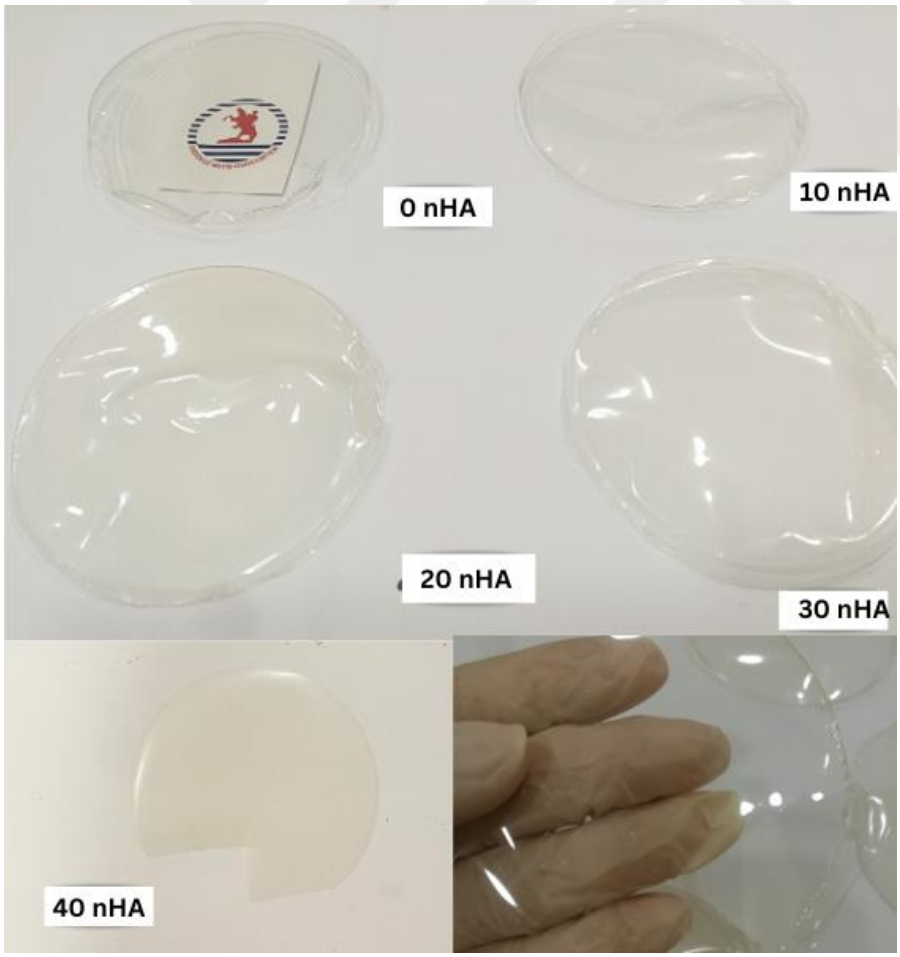


Figure 2.8. CS/PVA/PVP films with different % of nHA

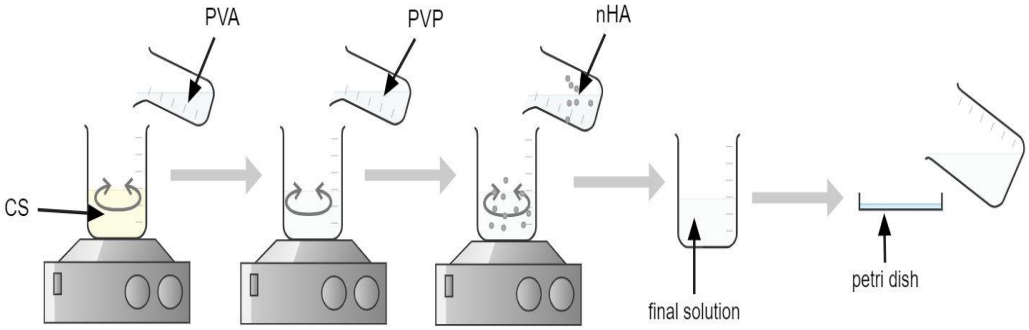


Figure 2.9. Schematic of the preparation process

### 2.2.2. Drug loading

To fabricate the drug-loading films containing 10 mg of nHA, the choice of using nHA at a concentration of 10 mg was based on its swelling behavior. the CS/PVA/PVP/nHA solution was prepared according to the aforementioned method. Quercetin was dissolved in ethanol at a concentration of 10 mg/mL, Figure 2.10.

Figure 2.10. Quercetin dissolved in ethanol

Once the drug had completely dissolved, 250 µL of the solution was slowly added to the hydrogel solution and stirred for 30 minutes. Figure 2.11 depicts the final solution loaded with quercetin.

Figure 2.11.Quercetin loaded in CS/PVA/PVP/nHA solution

The film was synthesized using the same method mentioned previously, and Figure 2.12 illustrates the films loaded with quercetin.

Figure 2.12. CS/PVA/PVP/nHA film loaded with Quercetin

## 2.3. Characterization Methods

### 2.3.1. Thermogravimetric Analyses (TGA)

To investigate the degradation profile of the hydrogel samples, their thermogravimetric analysis (TGA) was carried out using the TA Instruments SDT Q600 instrument. The weight loss of the hydrogel samples was measured as they were heated up to 800°C under $N_2$ flow at a heating rate of 20°C/min.

Figure 2.13.Thermogravimetric analysis device.

### 2.3.2. Differential Scanning Calorimetry (DSC)

To determine the thermal properties of gels, the DSCQ2000 Device is a Differential Scanning Calorimetry (DSC) instrument used. The device can measure thermal transitions over a temperature range of -90 °C to 550 °C in a controlled nitrogen atmosphere using an aluminum pan sample holder. The heating rate is 10.00°C/min, allowing for efficient and accurate measurements.

Figure 2.14. Differential Scanning Calorimetry device

### 2.3.3. Antibacterial Study

The disc diffusion method was used to determine the synthetic hydrogels' antibacterial capabilities. First, 200 µL of bacterial medium containing both Gram-positive (*S. aureus* and *B. subtilis*) and Gram-negative (*E. coli* and *S. enterica*) bacteria

were inoculated onto Mueller Hinton Agar plates. On the agar plates, wells were drilled, and 100 μL of the synthetic hydrogels were put into the wells. The antibacterial activity was then determined by measuring the inhibition zone surrounding the hydrogel disc after the plates had been incubated at 37 °C for 24 hours. The conventional antibiotic rifampicin, which acted as a positive control, was used to compare the outcomes.

### 2.3.4. Scanning Electron Microscopy (SEM)

JEOL JSM 7001 FEG gun scanning electron microscopy was used to investigate morphology of synthesized films, Figure 2.15. The operating voltage of the SEM is 0.1 kV to 30 kV with a magnification of 10x—1000000x. It is equipped with 5-axis motorized eucentric goniometer and, samples with 200 mm diameter and 48 mm height can be analyzed. It has secondary electron (SE), back scattered electron (BSE), scanning transmission electron microscopy in an SEM (STEM-in-SEM), 80 $mm^2$ active area energy dispersive X-ray spectroscopy (EDS), wavelength dispersive spectroscopy (WDS) and electron backscatter diffraction (EBSD) detectors.

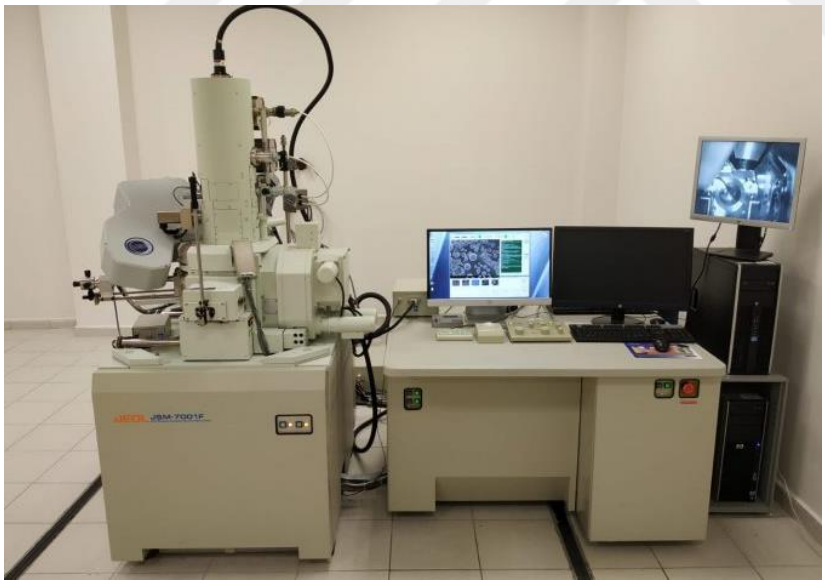

Figure 2.15. Scanning Electron Microscopy

### 2.3.5. Fourier Transform Infrared (FTIR)

The device used for the Fourier transform infrared spectroscopy (FTIR) tests of the samples is equipped with a Digitec detector and a DLATGS sensor, capable of recording spectra with a resolution of 0.9 $cm^{-1}$ and wavelength accuracy of 0.01 $cm^{-1}$. The device has a spectral range of 4000 $cm^{-1}$ to 400 $cm^{-1}$ and operates at room temperature.


Figure 2.16. Fourier transform infrared spectroscopy

### 2.3.6. Mechanical Test

The Zwick/Z010 Universal Testing Machine was utilized to examine the mechanical characteristics of the hydrogel films. The assessment was conducted at room temperature, employing a crosshead speed of 100 mm/min, in adherence to the guidelines outlined in ASTM D412.

### 2.3.7. Swelling Test

The weight difference method was employed to evaluate the swelling behavior of the synthesized films. The films were sliced into small and uniform pieces and then submerged in 15 mL of phosphate buffer solution (PBS). Afterward, the films were taken out of the PBS and dried before being weighed, at specific time intervals (every 10 minutes). The pH of the swelling medium was maintained at 7.4. Equation (1) was utilized to assess the swelling at equilibrium, which is calculated as the difference between the weight of the swelled blends ($W_S$) and the weight of the dry blends ($W_D$).

Equilibrium swelling % = $W_S – W_D / W_D * (100)$ (Sullad et al., 2010)

### 2.3.8. Drug release test

The study involved the suspension of polymeric films measuring 1×1 cm in 50 ml of phosphate buffer saline medium (7.4 pH) at 37 °C for 300 minutes to investigate the drug release behavior in vitro. Sampling was performed at regular 15-minute intervals by withdrawing 1 ml of samples using a pipette, and the same volume was replenished after each sampling to account for the total amount of drug released over time, the system was controlled as shown in Figure 2.17. The amount of drug released

was measured using a UV-Vis spectrophotometer Figure 2.18, specifically by measuring the absorbance at a wavelength of 377 nm.

The calculation of the cumulative drug release percentage involves dividing the total amount of drug released up to a certain time point by the total amount of drug present in the original hydrogel and multiplying the result by 100, expressed in the following equation:

Cumulative drug release (%) = (Total amount of drug released up to time t / Total amount of drug in the original hydrogel) x 100 (Rossi et al., 2017)

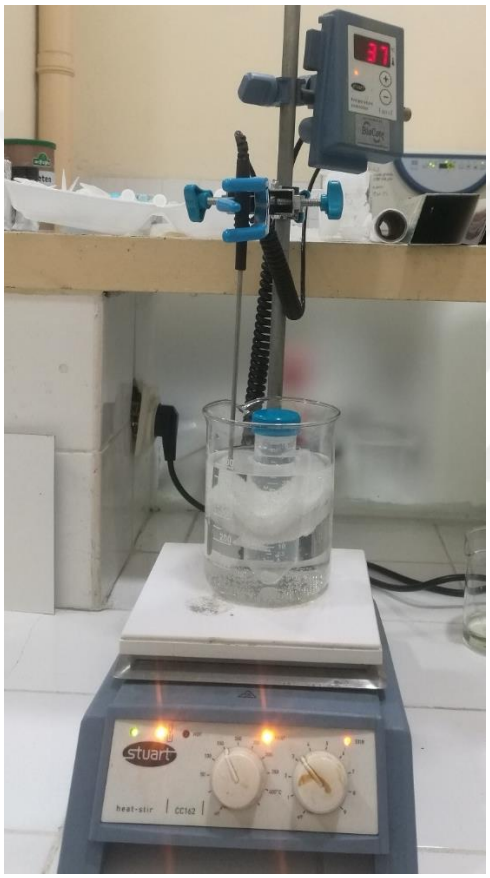


Figure 2.17. Drug release test

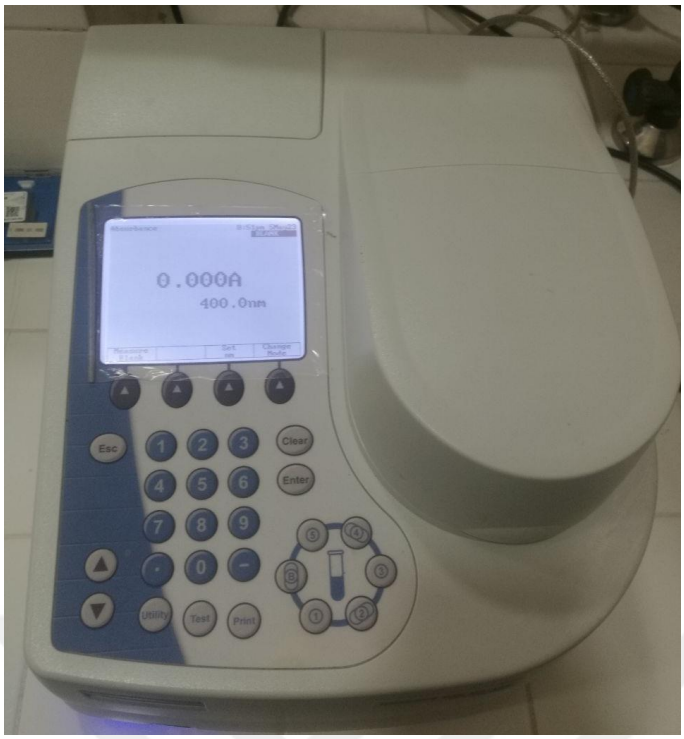


Figure 2.18. UV-Vis spectrophotometer

In addition, the drug entrapment efficiency is determined using a standard graph for Quercetin. To prepare this graph, a Quercetin drug solution is made at various concentrations using a serial dilution method. The graph shown below in Figure 2.19 is then used to calculate the drug entrapment efficiency of the hydrogel film.

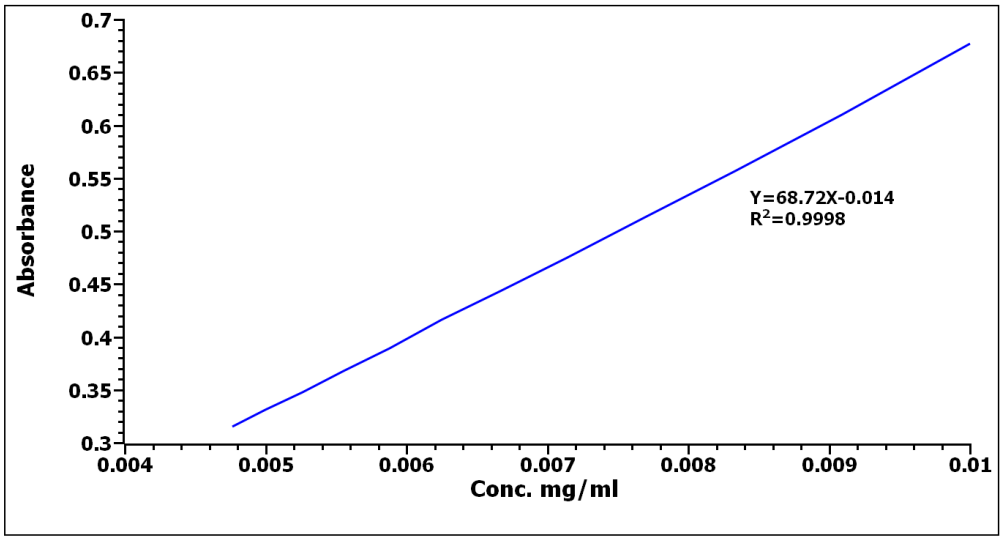


Figure 2.19. Calibration curve of the drug release

# 3. RESULTS AND DISCUSSION

## 3.1. Antibacterial Results

The antibacterial activity of the hydrogel samples was tested using the disc diffusion method against Gram-positive (*S. aureus* and *B. subtilis*) and Gram-negative (*E. coli* and *S. enterica*) strains of bacteria. Table 3.1 show the results.

Table 3.1. Data represent the antibacterial activity (zone of inhibition)

| Sample code | zone of inhibition (mm) | | | |
|---|---|---|---|---|
| | *S. Aureus* | *B. Subtilis* | *E. Coli* | *S. Enterica* |
| CS | 16±1 | 11 | 7 | 7 |
| PVA | 7 | 0 | 0 | 0 |
| PVP | 7 | 0 | 0 | 0 |
| CS/PVA/PVP/0nHA | 25 | 30±5 | 17±1 | 14 |
| CS/PVA/PVP/10nHA | 23±1 | 28±3 | 28±9 | 13±1 |
| CS/PVA/PVP/20nHA | 27±5 | 33±8 | 21±3 | 14±1 |
| CS/PVA/PVP/30nHA | 34±8 | 33±11 | 20±4 | 15±2 |
| CS/PVA/PVP/40nHA | 31±9 | 27±8 | 17±4 | 10 |
| Antibiotic (Rifampicin) | 30 | 26±2 | 33±1 | 24±2 |

*S. aureus* and *B. subtilis* are Gram-positive bacteria. They have a thick peptidoglycan layer in their cell wall, and when exposed to a Gram stain, this layer turns purple. Gram-negative bacteria include *E. coli* and *S. enterica*, their unique staining abilities are caused by a lipopolysaccharide-containing outer membrane and a thinner peptidoglycan layer. They lose the crystal violet-iodine complex when exposed to a Gram stain and instead, acquire a pink hue after being counterstained with safranin (Rasool, Ata, Islam, et al., 2019).

The antibacterial properties of chitosan attracted a lot of interest. It is proposed that the ammonium ions at the positive ends of chitosan molecules are what provide their antibacterial properties. The ammonium ions may interact with the bacterial cell wall when chitosan is present in a hydrogel, disrupting it and causing cell death. By providing a prolonged release of the biopolymer and extending its contact time with the bacteria, the hydrogel matrix can also increase the antibacterial activity of chitosan (Chung & Chen, 2008; Wang et al., 2012).

While the antibacterial properties of nano-hydroxyapatite (nHA) against Gram-positive bacteria are attributed to the negative ions present in both phosphate groups and calcium ions. By interacting with the bacterial cell wall, the phosphate groups on the surface of nHA can damage the cell wall's integrity and cause bacterial death. Additionally, by affecting the permeability of the bacterial cell membrane and

impairing cellular processes, the release of calcium ions from nHA may also contribute to its antibacterial activity (Phatai et al., 2019).

As mentioned, these kinds of bacteria have a single membrane consisting of a thick, peptidoglycan-based cell wall. When nanohydroxyapatite (nHA) comes into contact with these bacteria, it generates reactive species such as hydroxyl radicals (OH), hydrogen peroxide ($H_2O_2$), and superoxide anions ($O^{2-}$). These reactive species can penetrate the bacterial cell wall and cause damage to important cellular components. In addition, the needle shape of nHA can also help to physically destroy the bacterial cell wall, further enhancing its antibacterial activity. Reactive oxygen species (ROS) generated by nHA have the potential to damage the peptidoglycan of bacteria, leading to changes in their morphology and susceptibility to other antibacterial agents. Furthermore, ROS can also disrupt bacterial metabolic processes, leading to reduced viability and growth inhibition (Xu et al., 2012).

The differences in the structure as well as the chemical composition of the cell surface can be utilized to clarify why these two kinds of bacteria react differently with the hydrogel (Prakash et al., 2019).

As was pointed out, Gram-negative bacteria have a thinner peptidoglycan layer and an outer membrane containing lipopolysaccharides, making them less susceptible to some antibacterial agents than Gram-positive bacteria. However, the hydrogel film's antibacterial properties can be enhanced against this kind by the release of $Ca^{2+}$ and $PO4^{3-}$ ions from nanohydroxyapatite (nHA). These ions can interact with the negatively charged surface of Gram-negative bacteria, destabilizing their outer membrane and leading to increased permeability and ultimately cell death. Additionally, the sustained release of these ions from the hydrogel film can provide a long-lasting antibacterial effect, preventing the growth and colonization of Gram-negative bacteria in the surrounding environment (Pal et al., 2007; Selvakumar et al., 2016).

### 3.2. Differential Scanning Calorimetry Analysis

Figure 3.1 shows the DSC behavior of the hydrogel samples. The outcomes from a single heating-cooling cycle have been recorded, with the temperature ranges for the heating and cooling cycles being 25°C to 200.00°C and 200.00°C to -60.00°C, respectively.

Since CS-PVA-PVP hydrogels have a high capacity for water absorption and residual water can remain in the hydrogel even after drying, the decrease in the cooling curve is caused by the residual water in the hydrogel. The leftover water may freeze and release heat during the DSC cooling cycle, producing a positive peak on the cooling curve. The sublimation of the frozen water may occur while the chilling process proceeds, resulting in a reduction in heat flow and a downward slope of the curve. which was well correlated with the TGA result (Zulfiqar et al., 2020).

For the heating curves, all five hydrogel film samples show a wide endothermic peak indicating a melting event. The melting temperature for the samples ranges from 86°C to 107°C, with the 20 mg of the nano-hydroxyapatite sample having the highest melting temperature. The heat capacity at the full melting point varies between the samples, with values ranging from -1.252 to -1.67. Interestingly, the sample with the highest heat capacity at the full melting point (sample 20 nHA) also has the highest melting temperature. This suggests that the addition of nano-hydroxyapatite may increase the strength of the intermolecular forces within the hydrogel network, leading to a higher energy requirement for melting and a higher heat capacity at the full melting point (Zhu et al., 2018).

In contrast, the sample with the lowest heat capacity at the full melting point is the sample with 40 mg of the nano-hydroxyapatite. This suggests that the intermolecular forces within this sample are weaker, requiring less energy to overcome and resulting in a lower heat capacity at the full melting point, this can be explained by the fact that the thermal behavior of a hydrogel can be enhanced by the incorporation of a specific percentage of nano-hydroxyapatite. However, an excessive amount of nano-hydroxyapatite can generate defects in the polymer matrix, causing a disruption in the hydrogen bonding and resulting in a reduction of the thermal stability of the hydrogel. Consequently, the concentration of nano-hydroxyapatite should be optimized to attain the desired properties of the hydrogel.

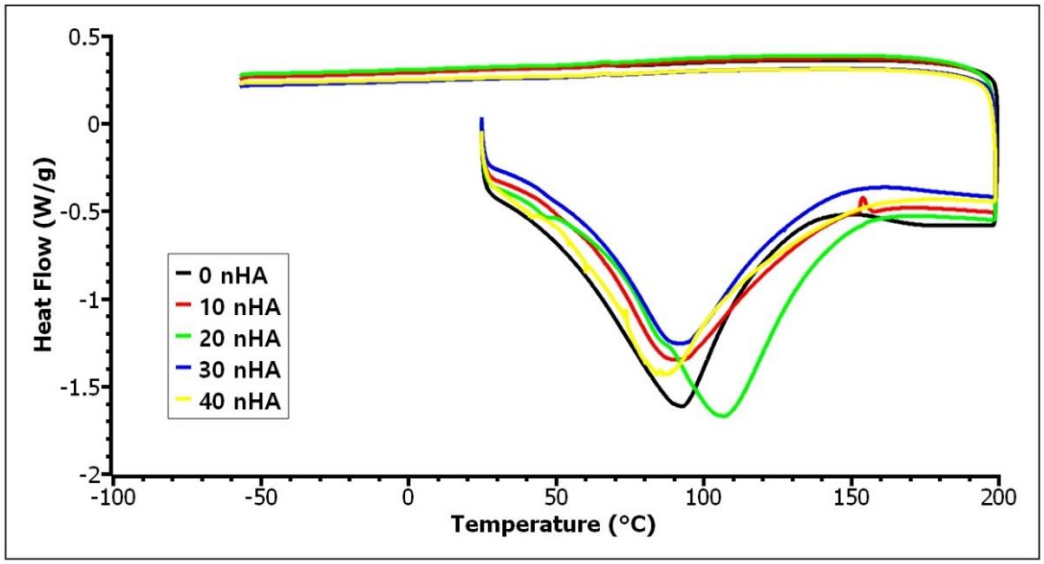


Figure 3.1.The DSC behavior of the hydrogel samples.

### 3.3. Thermogravimetric Analyses

The thermograms of hydrogel samples shown in Figure 3.2 were analyzed using thermogravimetric analysis (TGA) to evaluate the influence of nHA on the thermal stability of the hydrogels. The results of the TGA analysis showed that the degradation of the hydrogels could be divided into three stages based on temperature ranges. The first stage, which occurred at temperatures between 28 and 270°C, was attributed to the evaporation of adsorbed water molecules from the hydrogel network. As the temperature increases, weak chemical bonds such as -OH within the hydrogel matrix start to break down, leading to the second stage of degradation between 270 and 420°C. This stage is associated with the fragmentation of the hydrogel backbone and the release of small molecules such as water and carbon dioxide. The third stage of degradation, which occurs at temperatures between 420 and 788°C, is characterized by the fragmentation of the hydrogel framework into smaller molecules. This stage is associated with the cleavage of stronger chemical bonds such as C-C and C-O bonds within the hydrogel network (Qi et al., 2019).

Results indicate that the hydrogel without the incorporation of nano-hydroxyapatite experienced a higher weight loss percentage during the three degradation stages in comparison to the hydrogel films that contain varying amounts of nano-hydroxyapatite. These results suggest that the addition of nano-hydroxyapatite has a significant effect on the thermal stability of the hydrogel films, potentially due to the interactions between the nano-hydroxyapatite and the hydrogel matrix. Such

interactions may influence the strength of the hydrogen bonding in the polymer matrix, leading to the enhanced thermal stability of the hydrogel films. Further optimization of the concentration of nano-hydroxyapatite can potentially enhance the thermal stability of the hydrogel films.

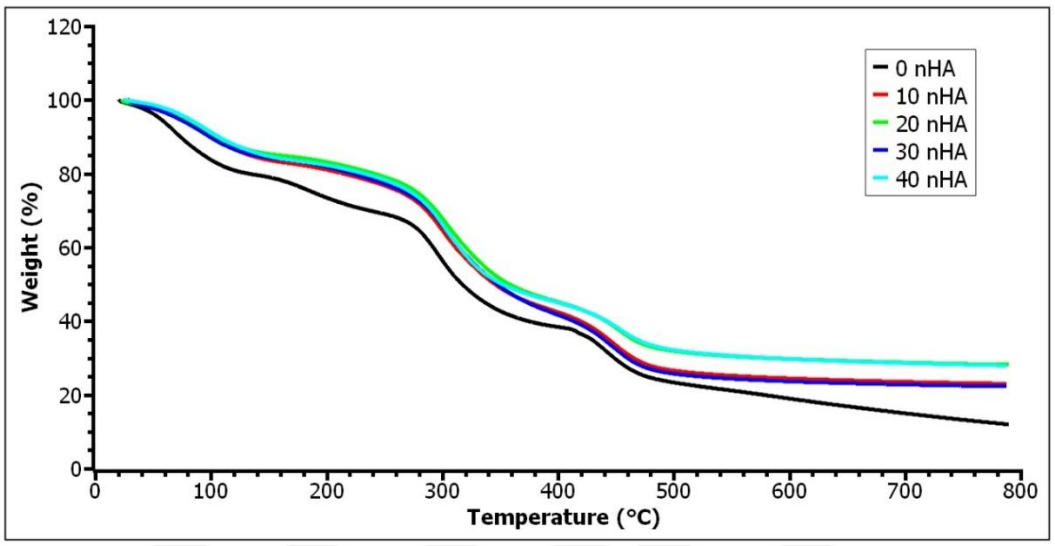


Figure 3.2. Thermogravimetric behavior

### 3.4. Fourier Transform Infrared (FTIR) Analysis

Chitosan's IR characterization shows a strong peak at 3363 cm-1 and 3293 $cm^{-1}$ corresponding to the stretching vibration of O-H and N-H bonds. These are characteristic of chitosan's primary amino groups and hydroxyl groups. Additionally, the absorption bands at 2872 $cm^{-1}$ correspond to the stretching vibration of C-H bonds, likely from the chitosan's acetyl group, and are commonly found in other polysaccharides (Melo-Silveira et al., 2012; Wolkers et al., 2004). The band at 1587 $cm^{-1}$ in the IR spectrum corresponds to the amide II vibration, coupling N-H bending and C-N stretching (Lim & Hudson, 2004). Peaks at 1420 $cm^{-1}$ and 1375 $cm^{-1}$ correspond to the C-H bond bending in the CH3 group of the acetyl group and the CH2 group of the chitosan backbone, respectively. The stretching vibration of the C-N bond in the amide III bands of chitosan corresponds to 1320 $cm^{-1}$, while 1150 $cm^{-1}$ corresponds to the stretching vibration of the C-O bond in the glycosidic bond of chitosan. The sharp peak at 1025 $cm^{-1}$, with small peaks at 1060 $cm^{-1}$ and 989 $cm^{-1}$, corresponds to the stretching vibration of the C-O-C bond in the glycosidic bond of chitosan and is commonly found in chitosan samples reported by others (C. Song et

al., 2013; Vino et al., 2012). Finally, the bonds at 941 $cm^{-1}$ and 839 $cm^{-1}$ correspond to the bending vibration of the C-H bond in the CH2 group of the chitosan backbone, the C-H bending in the pyranose ring, and the C-H rocking in the glucosamine unit of chitosan, respectively (C. Song et al., 2013).

The IR spectrum of PVA shows a wide peak at 3293 $cm^{-1}$, which corresponds to the stretching vibration of O-H (hydroxyl) groups. The two peaks observed at $cm^{-1}$ and 2909 $cm^{-1}$ correspond to the asymmetric and symmetric stretching vibrations of the CH2 (methylene) groups, respectively. The peak observed at 1731 $cm^{-1}$ is due to the C=O (carbonyl) stretching vibration in PVA, indicating the presence of acetyl groups (Jipa et al., 2012).

The bending vibration of the -$CH_2$- groups is observed at 1422 $cm^{-1}$, while the bending vibration of the C-H groups is observed at 1373 $cm^{-1}$. The bending vibration of C-O-C (ether) groups is observed at 1326 $cm^{-1}$, while the stretching vibration of C-O (ether) groups is observed at 1241 $cm^{-1}$ (Jipa et al., 2012).

The band observed at 1088 $cm^{-1}$ is due to the stretching vibration of C-OH (alcohol) groups in PVA, while the band observed at 945 $cm^{-1}$ is due to the rocking vibration of CH2 groups. The peak observed at 841 $cm^{-1}$ is due to the wagging vibration of CH (methine) groups in PVA, providing further evidence of the presence of acetyl groups. Finally, the band observed at 474 $cm^{-1}$ is due to the wagging vibration of the C-H bonds in the acetate units or the rocking vibration of the C-O-C bonds in the pyranose ring (Jipa et al., 2012).

The infrared (IR) spectrum of polyvinylpyrrolidone (PVP) a broad peak at approximately 3414 $cm^{-1}$ corresponds to the stretching vibration of the hydroxyl (OH) group and/or the N-H group of the pyrrolidone ring in the PVP (Abdelrazek et al., 2010). Additionally, two peaks at around 2951 $cm^{-1}$ and 2882 $cm^{-1}$ are attributed to the stretching vibrations of the C-H bonds in the methylene (CH2) groups of PVP (Abdelghany et al., 2016). A sharp peak at approximately 1646 $cm^{-1}$ is due to the stretching vibration of the C=O group (Abdelrazek et al., 2010), while peaks at 1493 $cm^{-1}$ and 1017 $cm^{-1}$ correspond to the characteristic vibrations of the C=N and C-N groups, respectively (Abdelghany et al., 2016). Additionally, bending vibrations of CH and CH2 groups in PVP are associated with peaks at 1460 $cm^{-1}$, 1421 $cm^{-1}$, and 933 $cm^{-1}$, while the bending vibration of the C-H group in the CH2 group of PVP is

assigned to a peak at 1372 $cm^{-1}$. Peaks at 1285 $cm^{-1}$, 1272 $cm^{-1}$, and 894 cm-1 correspond to the bending and out-of-plane bending vibrations of the C-H group in the CH2 group of PVP (Abdelghany et al., 2016). Further, peaks at 1228 $cm^{-1}$ and 1002 $cm^{-1}$ are attributed to C-C stretching and/or CH2 deformation and the stretching vibration of the C-C bond in the pyrrolidone ring, respectively. Finally, the stretching and out-of-plane bending vibrations of the pyrrolidone ring in PVP are associated with peaks at 1169 $cm^{-1}$, 1073 $cm^{-1}$, 842 $cm^{-1}$, 735 $cm^{-1}$, 646 $cm^{-1}$, and 569 $cm^{-1}$ (Zidan et al., 2019).

The spectrum of nanohydroxyapatite shows one such band is located at 3571 $cm^{-1}$ and corresponds to the O-H stretching vibration of hydroxyl groups present in the nanohydroxyapatite. Another band at 1089 $cm^{-1}$ corresponds to the P-O bending mode of the phosphate groups in the nanohydroxyapatite (Venkatasubbu et al., 2013).

A well-defined and sharp absorption band at 1023 $cm^{-1}$ corresponds to the P-O stretching mode of the phosphate groups in the nanohydroxyapatite, which is indicative of a highly crystalline material. A band peak at 963 $cm^{-1}$ is attributed to the carbonate group vibration in the nanohydroxyapatite (Venkatasubbu et al., 2013).

Additional bands at 628 $cm^{-1}$ and 472 $cm^{-1}$ may correspond to the phosphate ($PO4\ 3-$) group, while the bands at 600 $cm^{-1}$ and 561 $cm^{-1}$ correspond to the stretching vibrations of the phosphate. These bands provide further information about the composition and structure of the nanohydroxyapatite and can be used to determine the degree of crystallinity and the presence of impurities or other substitutions (Prakash et al., 2019b).

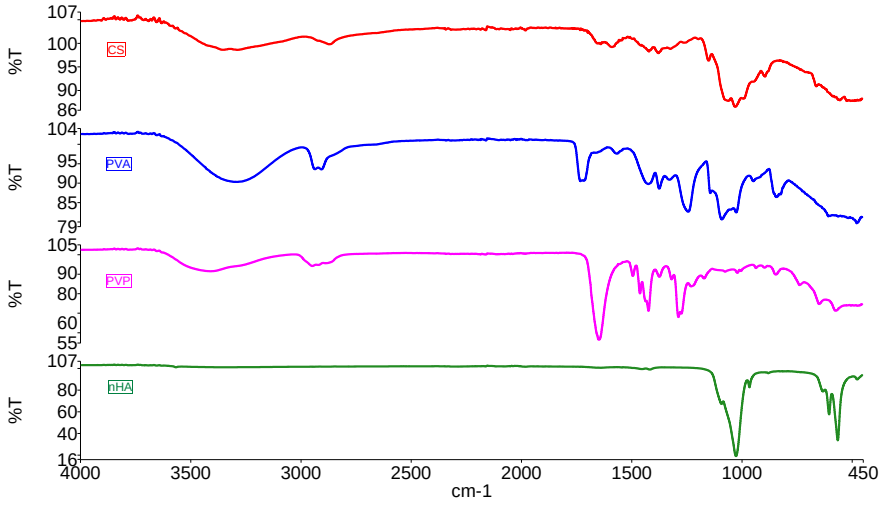


Figure 3.3. FTIR results of CS, PVA, PVP and nHA

The FTIR results of the hydrogel films show wide peaks at 3240, 3270, 3238, 3269, and 3270 for samples to the stretching vibration of O-H and N-H bonds, which are characteristic of the hydroxyl and primary amino groups of chitosan and the hydroxyl groups of PVA (Prakash et al., 2019b). The slight shift in the -OH stretching vibrations of the samples containing nanohydroxyapatite compared to the sample without nanohydroxyapatite could be due to the interaction between the hydroxyl groups in the nanohydroxyapatite and the polymer matrix.

The band at 2918 $cm^{-1}$ in all samples corresponds to the symmetric stretching vibration of -CH groups in the chitosan (Tripathi et al., 2012).

The bands at 1733 $cm^{-1}$ and 1734 $cm^{-1}$ for the hydrogel films with and without nanohydroxyapatite correspond to the carbonyl stretching vibrations (C=O) of the acetyl group in PVA. The peak at 1739 $cm^{-1}$ in the hydrogel film with 40 mg nanohydroxyapatite may also correspond to the carbonyl stretching vibrations of the acetyl group in PVA, but the shift to a slightly higher frequency could suggest that the acetyl group is interacting differently with the nanohydroxyapatite in this sample compared to the other samples with lower amounts of nanohydroxyapatite which could indicate that the presence of a higher amount of nanohydroxyapatite may be affecting the interaction between the polymer and the nanohydroxyapatite in the hydrogel film.

The band at 1650 $cm^{-1}$ in the FTIR spectra of all samples of the hydrogel film corresponds to the amide I band, which is primarily due to the stretching vibrations of the C=O bond in the peptide backbone of proteins and the N-H bond bending vibrations of the peptide bond. This suggests that there may be some protein-like structures present in the hydrogel film, possibly due to the presence of chitosan, which contains amino groups in its molecular structure. Alternatively, it could be due to the presence of proteins in any of the components used to prepare the hydrogel film, such as chitosan or nanohydroxyapatite. (Shakir et al., 2015) it is worth noting that the amide I band is often used as an indicator of the secondary structure of proteins, with different structures giving rise to characteristic peaks at different frequencies. However, in the case of the hydrogel film, the presence of multiple components makes it difficult to accurately identify any secondary structure features in the amide I band.

The band at 1555 $cm^{-1}$ in the FTIR spectra of all samples of the hydrogel film corresponds to the amide II band, which is primarily due to the bending vibrations of

the N-H bond and stretching vibrations of the C-N bond in the peptide backbone of proteins. Similar to the amide I band at 1650 $cm^{-1}$, the presence of the amide II band suggests the presence of protein-like structures in the hydrogel film, possibly due to the presence of chitosan, which contains amino groups in its molecular structure, or the presence of protein in any of the components used to prepare the hydrogel film (Shakir et al., 2015).

The band at around 1408-1416 $cm^{-1}$ in the FTIR spectra of the hydrogel film corresponds to the bending vibrations of the carboxylate group (COO-) in the chitosan molecule. The slight variation in the frequency of this peak for different amounts of nanohydroxyapatite suggests that the interaction between chitosan and nanohydroxyapatite may be affected by the concentration of nanohydroxyapatite. It can also correspond to the bending vibration of the C-H bond in the alkyl groups of chitosan, PVA, and PVP since the C-H bending vibration in the alkyl groups of chitosan, PVA, and PVP can occur in the range of 1400-1450 $cm^{-1}$ (Shakir et al., 2015).

It is possible that the peak at 1291 $cm^{-1}$ in the FTIR spectra of the hydrogel film may also correspond to the stretching vibration of the C-N bond in the amide III bands of chitosan and PVP. The amide III bands are known to appear in the region of 1200-1350 $cm^{-1}$ in the FTIR spectra of proteins and other compounds containing amide groups (Böker et al., 2023).

A band at 1077 $cm^{-1}$ in the FTIR spectra of the hydrogel film is likely to correspond to the stretching vibration of the C-O bond in the saccharide ring of chitosan and PVA. The saccharide ring of chitosan and PVA contains several oxygen atoms that can participate in C-O bond formation that may be overlapped with phosphate, resulting in an absorption peak in this region. Changes in the intensity or position of this peak could indicate variations in the degree of saccharide ring substitution (Rajiv Gandhi et al., 2011).

The band at 1020 $cm^{-1}$ is a shift of IR adsorption bands towards lower wavenumber from pure chitosan to composite hydrogel suggesting the formation of hydrogen bonding between CS and nHA (Peng et al., 2016a). It also could correspond to the P-O stretching mode of the phosphate groups in the nanohydroxyapatite.

The band at 647 $cm^{-1}$ and 559 $cm^{-1}$ in the hydrogel film's FTIR spectra corresponds to the O-P-O group's bending vibration in the nanohydroxyapatite, for the

hydrogel without nanohydroxyapatite (Peng et al., 2016b), it is possible that the bands due to the presence of PVP. The band at 647 $cm^{-1}$ is a characteristic peak for the C-H out-of-plane bending vibrations in aromatic rings, which are present in the PVP molecule. The band at 559 $cm^{-1}$ may correspond to the C-S stretching vibration in the thioether group (-S-) of PVP.

The identification of specific functional groups in a hydrogel composed of multiple materials can be challenging due to the overlapping vibrational bands in the Fourier-transform infrared (FTIR) spectra. In particular, when hydroxyapatite nanoparticles are added to a hydrogel that contains chitosan, PVA, and PVP, the resulting FTIR spectra can exhibit complex and overlapping bands that make it difficult to determine the specific bonds present in the sample.

It should be noted that the FTIR spectra of all hydrogel samples, with and without nanohydroxyapatite, exhibit similar peaks, with minor shifts observed in certain regions. These results suggest that the incorporation of nanohydroxyapatite had no significant effect on the molecular structure of the hydrogel. However, the observed differences in transmittance values indicate that the addition of nanohydroxyapatite had an impact on the intensity of the absorption peaks. This change in transmittance could be attributed to a variety of factors, including alterations in the concentration of the hydrogel matrix, variations in particle size, changes in the distribution or orientation of functional groups within the hydrogel matrix as a result of the presence of nanoparticles, or agglomeration of nanoparticles within the hydrogel, all of which can affect the transmittance of FTIR spectra. Moreover, the presence of nanoparticles can also influence light absorption, reflection, and scattering, which can further affect the transmittance of the hydrogel.

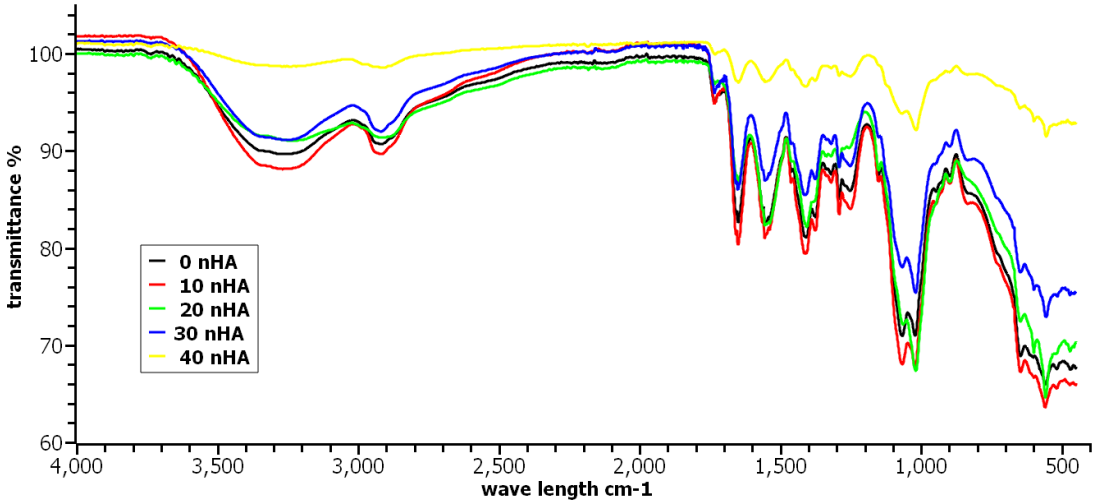


Figure 3.4. FTIR results of hydrogel films

### 3.5. Scanning Electron Microscopy

SEM SE images of parepared samples are seen in Figure 3.6a-e. The surface of the sample without nHA is non-porous and smooth, as seen in Figure 3.5 a. The surface of the sample 10 nHA (b) is similar to the surface of the sample 0 nHA. nHA is completely dispersed. Some nHA particles can be seen on the surface of the sample 20 nHA. nHA particles are dispersed well and there is no agglomeration. However, the surfaces of the sample 30 nHA (d) and 40 nHA (e) indicate that there is agglomeration.

In order to prove the existence of nHA in the samples, the samples were also analysed by EDS. In the EDS spectrum P Kalpha peak is seen. This indicates that particles are nHA.

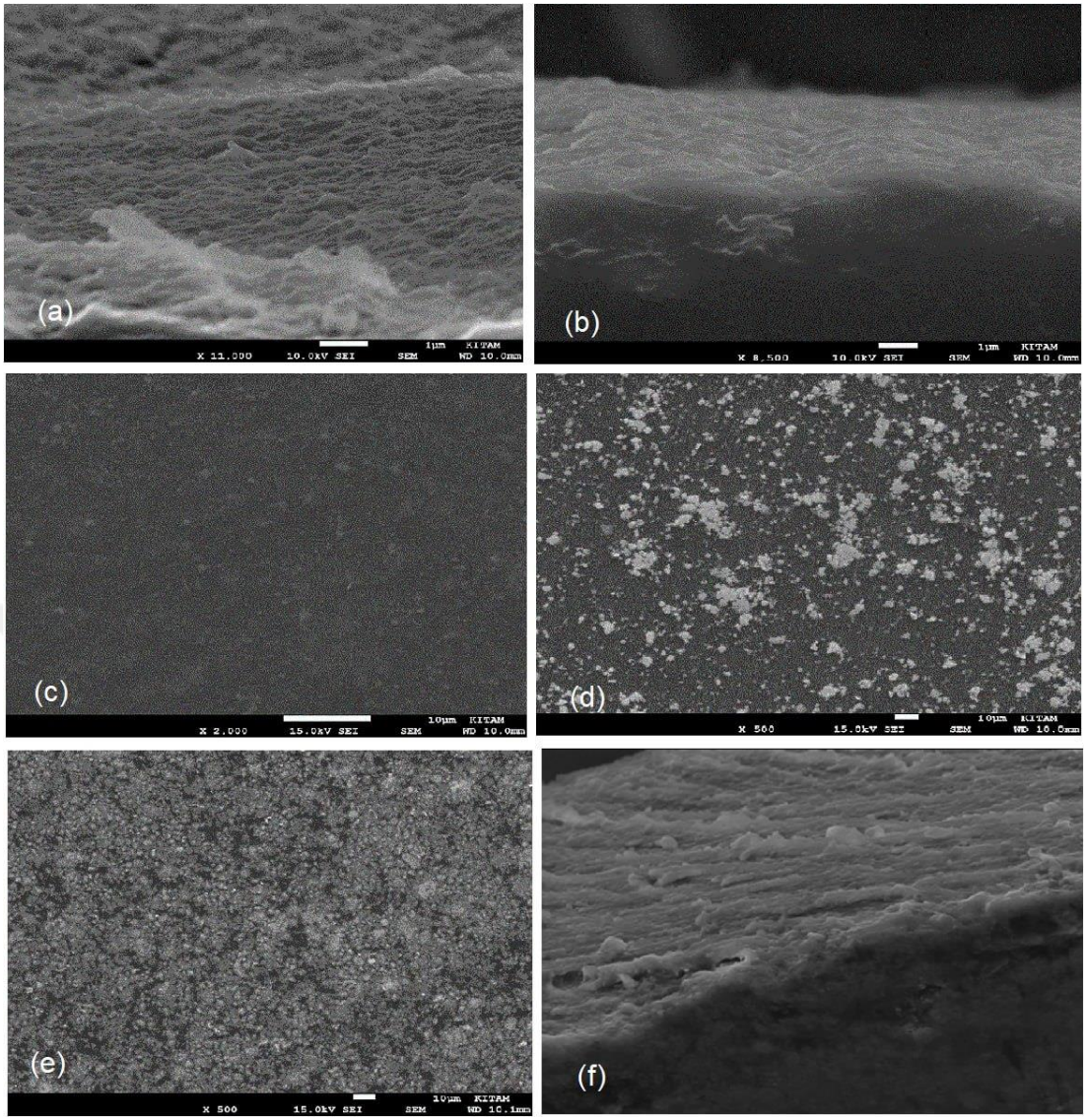


Figure 3.5. SEM images of the films; (a) the surface of the sample 0 nHA (b) the surface of the sample 10 nHA (c) the surface of the sample 20 nHA (d) the surface of the sample 30 nHA (e) the surface of the sample 40 nHA.

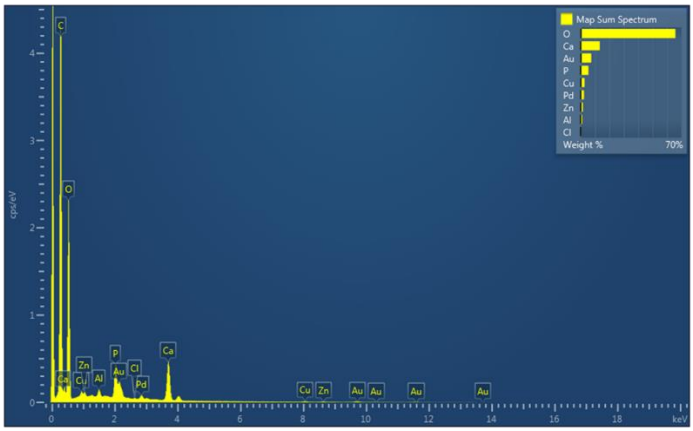


Figure 3.6 EDS analysis

### 3.6. Mechanical Test

Based on the result provided by the mechanical test shown in Figure 3.7 and Table 3.2 it could be observed that force at break and elongation at break increase with the increase of nHA, this means that as the amount of nHA in the hydrogel increases, the force required to break the hydrogel and the extent to which it can elongate before breaking also increase. This indicates an improvement in the mechanical strength and ductility of the hydrogel. The presence of nHA particles can reinforce the hydrogel matrix and enhance its resistance to deformation and fracture (Prakash et al., 2019c).

Young's modulus values of samples decrease with the increase of nHA. Young's modulus is a measure of the material's stiffness or hardness. The decrease in Young's modulus with increasing nHA content suggests that the hydrogel films become less stiff. The incorporation of nHA particles may disrupt the polymer network, leading to a softer or more flexible hydrogel. The interaction between the nHA particles and the polymer matrix may not be optimal, leading to poor bonding or weak interfacial interactions. This can result in a compromised load transfer between the particles and the polymer matrix, leading to reduced mechanical properties, this result has been also proved in FTIR results or the addition of nHA may interfere with the formation or stability of the polymer network within the hydrogel. This disruption can affect the overall integrity and mechanical strength of the hydrogel (Deng et al., 2020).

The overall trend of decreasing Young's modulus and the mentioned increase in elongation at break indicates that the hydrogels become softer or more pliable upon the addition of nHA. This softening effect can be desirable in certain applications where flexibility or tissue-like properties are desired.

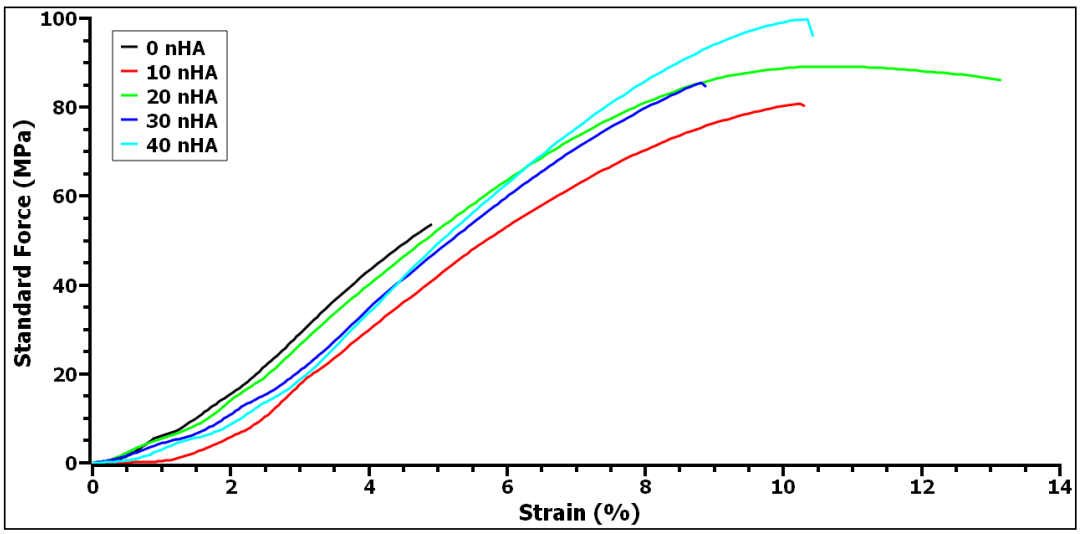


Figure 3.7.Stress-strain curves of the films

Table 3.2. Results of the tensile test

| Sample code | Yong modulus | Force $_{break}$ | Elongation $_{break}$ |
|---|---|---|---|
| | MPa | MPa | % |
| CS/PVA/PVP/0nHA | 1041±370.8 | 62.3±34 | 8.29±3.14 |
| CS/PVA/PVP/10nHA | 590±215.4 | 42.3±34 | 22±30.4 |
| CS/PVA/PVP/20nHA | 678.9±319.3 | 64.8±37.4 | 11.8±8.5 |
| CS/PVA/PVP/30nHA | 609±99.4 | 79.5±9.2 | 9.5±2.1 |
| CS/PVA/PVP/40nHA | 662.5±134.4 | 85.4±10 | 9.7±1.2 |

### 3.7. Swelling Test

The swelling behavior of the film is shown in Figure 3.8. For the sample without nHA, the swelling ratio increases from 242% at 10 minutes to 444% at 100 minutes. After 100 minutes, the swelling ratio decreases slightly to 434% at 110 minutes then decreased again to 398% at 120 minutes and remains constant. Overall, the swelling behavior of this hydrogel film demonstrates that it has good swelling capacity and can absorb significant amounts of water or other solvents. The gradual and continuous increase in swelling ratio suggests that the hydrogel has a stable and consistent structure that can maintain its integrity under prolonged exposure to solvent. However, the slight decrease in swelling ratio after 100 minutes indicates that the hydrogel may reach a saturation point where it can no longer absorb more solvent.

The film with 10 mg of nHA has a significant and rapid increase in weight or volume as the time in the PBS solution increases. The swelling ratio starts at 280% at 20 minutes and increases rapidly to 585% at 100 minutes, where it remains constant until 140 minutes. The high swelling ratio indicates that the hydrogel film has a high-

water uptake capacity, which may be attributed to the presence of hydrophilic groups in chitosan, PVA, and PVP, as well as the nanoporous structure of nanohydroxyapatite.

The film with 20 mg of nHA has a gradual increase in weight or volume as the time in the PBS solution increases. The swelling ratio starts at 215% at 20 minutes and increases gradually to 470% at 120 minutes, where it remains constant until 130 minutes and slightly decreases to 466% at 140 minutes. This film shows a gradual and sustained increase in the swelling ratio

The film with 30 mg of nanohydroxyapatite showed a gradual increase in swelling over time. The hydrogel initially swelled by 213% after 10 minutes and continued to increase to a maximum swelling ratio of 484% after 120-130 minutes. After the maximum swelling was reached, the hydrogel remained relatively stable, with a slight decrease in swelling to 480% after 140 minutes.

For the hydrogel film with 40 mg of nanohydroxyapatite, the swelling behavior is characterized by an initial low swelling ratio that gradually increases with time until it reaches a maximum value. The hydrogel swells the least at 10 and 30 minutes with swelling ratios of 183% and 183%, respectively. However, at 50 minutes, the swelling ratio increases to 242%, and the hydrogel continues to swell until it reaches a maximum value of 425% at 110 minutes and then started to decrease reaching 390% at 140 minutes.

Compared to the hydrogels with lower concentrations of nanohydroxyapatite, the hydrogel with 40 mg of nanohydroxyapatite has a slower initial swelling rate but reaches approximately a similar maximum swelling ratio. The addition of nanohydroxyapatite appears to delay the onset of swelling and reduce the overall rate of swelling, which may be due to the increased crosslinking density caused by the presence of the nanoparticles. Additionally, the hydrogels with nanohydroxyapatite generally exhibit higher swelling ratios than the hydrogel without nanohydroxyapatite. The amount of nanohydroxyapatite affects the swelling behavior of the hydrogels, with the hydrogel with 10 mg of nanohydroxyapatite exhibiting the highest swelling ratio, followed by the hydrogel with 20 mg of nanohydroxyapatite, and so on.

Overall, the appropriate selection of the quantity of nanohydroxyapatite (nHA) incorporated into hydrogel matrices plays a critical role in determining the resultant hydrogel's swelling behavior.

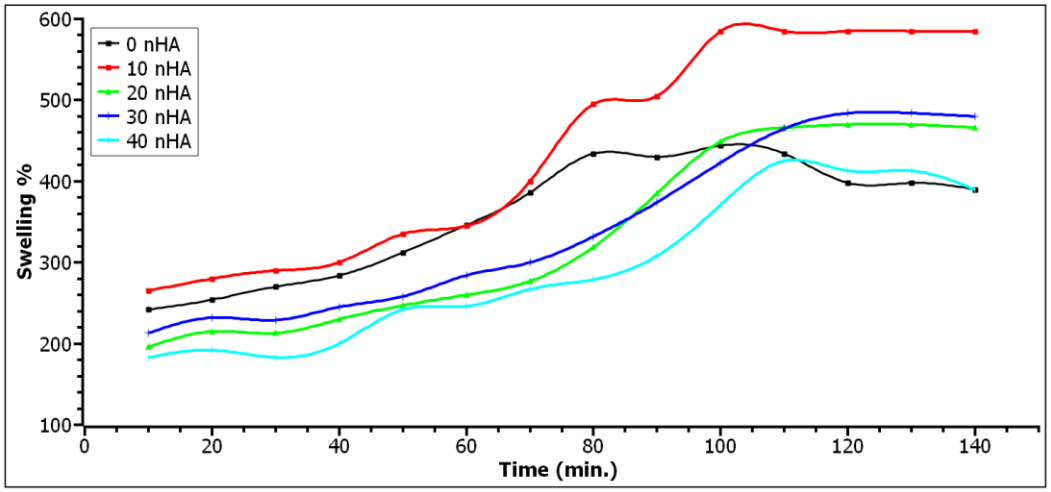


Figure 3.8. Swelling behavior of the film

### 3.8. Overview of Drug Release Result

Hydrogels have been widely used as drug release carriers due to their abundance of functional groups, biocompatibility with the in vivo environment, and ability to adapt to self-destructive degradation duration (Shi et al., 2019). These properties allow hydrogels to immobilize drugs and release them in a controlled manner through various mechanisms, such as simulated-controlled, diffusion-controlled, solvent-controlled, and degradation-controlled methods. Solvent-controlled strategies are further categorized into swelling-controlled and osmotic pressure-controlled modes. The drug release response in the investigated sample is predominantly governed by the swelling-controlled mechanism, which is directly influenced by the structural network of hydrogels. As hydrogels undergo swelling, this mechanism becomes a critical factor in drug release, their mesh size increases, and drug molecules are released through the diffusion mechanism (Son et al., 2017).

In our study, a hydrogel film with 10 mg of nanohydroxyapatite was selected for the loading of quercetin due to its swelling behavior and other favorable characterizations. When the release of quercetin molecules from the film was monitored, it resulted in an increase in absorbance, and the slow and steady release of the drug was attributed to molecular interactions such as hydrogen bonding and van der Waals interactions in the polymer matrix (Ata et al., 2020), the drug release profile of the film is shown in Figure 3.9.

The drug release behavior of the hydrogel film was then compared with its swelling behavior. It was observed that the swelling ratio of the hydrogel film

increased rapidly over the first hour, indicating that the hydrogel was reaching its maximum swelling capacity. This rapid increase in swelling ratio was followed by a plateau of around 400%, indicating that the hydrogel may not be able to absorb much more water. Similarly, the cumulative release of quercetin was slow and steady in the initial minutes, followed by a more rapid increase until it reached a plateau of around 74%. This indicates that the drug was being released from the hydrogel film as it swelled and absorbed water, but the rate of release was limited by the swelling behavior of the hydrogel.

Overall, the combination of the hydrogel film with nanohydroxyapatite and the drug quercetin has promising potential for controlled drug release, as the swelling behavior of the hydrogel can be utilized to regulate the release rate of the drug.

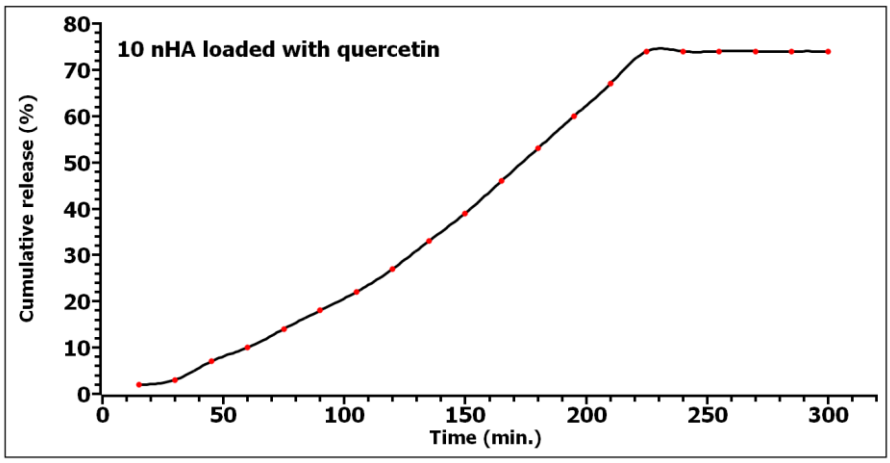


Figure 3.9. The drug release profile of 10 nHA film loaded with Quercetin

# 4. CONCLUSION

In this study, a pioneering approach was employed to synthesize biocompatible hydrogel films through the blending of natural and synthetic polymers, alongside the introduction of a nanoceramic material as a filler. By incorporating chitosan, Polyvinyl alcohol (PVA), Polyvinylpyrrolidone (PVP), and nano-hydroxyapatite (nHA), the films were successfully prepared via the solution casting method. The primary objective of this research endeavor was to develop a novel composite material that exhibits promising prospects for biomedical applications, while also unraveling the unique impact of nano-hydroxyapatite as a filler, renowned for its exceptional biomedical properties.

The findings of this investigation showcased remarkable antibacterial activity against gram-positive bacteria, surpassing the efficacy of the tested antibiotic upon the addition of nHA. While the antibacterial properties against gram-negative bacteria were also enhanced, they exhibited a comparatively lesser impact. These results unequivocally demonstrate the biocompatibility of the hydrogel films when subjected to bacterial media.

Thermographic analyses of the hydrogel samples revealed that films lacking the incorporation of nano-hydroxyapatite experienced heightened weight loss during the three degradation stages, as opposed to those containing varying concentrations of nHA. This observation suggests that the introduction of nano-hydroxyapatite exerts a substantial influence on the thermal stability of the hydrogel films. Further optimization of the nHA concentration holds the potential to enhance the thermal resilience of these films, thus paving the way for superior performance.

The Fourier-transform infrared (FTIR) spectra of all hydrogel samples, with and without nanohydroxyapatite, exhibited comparable peaks, albeit with minor deviations in certain regions. These outcomes indicate that the addition of nanohydroxyapatite does not significantly alter the molecular structure of the hydrogel. This finding can be perceived as advantageous for certain medical applications, as it ensures the preservation of the material's chemical integrity. However, it does impact other properties such as swelling behavior and stiffness. Consequently, the mechanical results indicate a reduction in Young's modulus, while an increase in elongation at break signifies a more pliable and flexible nature of the hydrogels upon the

introduction of nHA. Such a softening effect can prove beneficial in specific applications that demand flexibility or tissue-like characteristics.

The swelling behavior of the hydrogel films demonstrated excellent capacity in absorbing substantial quantities of water or solvents, exhibiting a stable and consistent structure capable of maintaining integrity even under prolonged exposure. Nonetheless, a slight decline in the swelling ratio after 100 minutes implies a saturation point where the hydrogel can no longer absorb additional solvent. This observation holds significance in medical applications, particularly concerning drug release mechanisms. Hence, meticulous selection of the nHA quantity incorporated into the hydrogel matrices assumes a critical role in determining the resultant swelling behavior.

Similarly, the drug release profile displayed a gradual and steady release of quercetin during the initial minutes, followed by a more accelerated increase until reaching a plateau of approximately 74%. This behavior signifies that the drug was released from the hydrogel film as it swelled and absorbed water. However, the release rate was influenced by the swelling characteristics of the hydrogel, emphasizing its pivotal role in controlled drug release applications.

To gain a comprehensive understanding of the impact of nanohydroxyapatite (nHA) on polymeric matrices, further investigations encompassing multiple factors are required. These studies aim to elucidate the nature of the interactions occurring between nHA and the polymeric matrix, as well as the resultant effects arising from these interactions. One crucial factor to consider is the percentage of nHA incorporated into the material, as it has been observed to exert a discernible influence on the properties of the prepared composite.

In addition to the nHA component, the combination of three polymers (chitosan, polyvinyl alcohol, and polyvinylpyrrolidone) has yielded intriguing outcomes. However, exploring the potential enhancements in the chemical structure or properties of the composite can be achieved by introducing suitable crosslinkers or alternative fillers. By incorporating appropriate crosslinkers, the chemical structure of the polymeric matrix can be reinforced, leading to potential improvements in mechanical and functional properties. Moreover, exploring different fillers can offer opportunities

to modify the composite's characteristics, tailoring it to specific applications or desired properties.

Conducting further studies in these areas will contribute to a more profound understanding of the behavior and performance of polymeric matrices when combined with nHA. Such investigations can shed light on the intricate interplay between various factors, enabling the optimization of composite materials for diverse applications in fields like biomedicine, materials science, and tissue engineering.

# REFERENCES


Abdelghany, A. M., Abdelrazek, E. M., Badr, S. I., & Morsi, M. A. (2016). Effect of gamma-irradiation on (PEO/PVP)/Au nanocomposite: Materials for electrochemical and optical applications. *Materials & Design*, *97*, 532–543. https://doi.org/10.1016/J.MATDES.2016.02.082

Abdelrazek, E. M., Elashmawi, I. S., & Labeeb, S. (2010). Chitosan filler effects on the experimental characterization, spectroscopic investigation and thermal studies of PVA/PVP blend films. *Physica B: Condensed Matter*, *405*(8), 2021–2027. https://doi.org/10.1016/J.PHYSB.2010.01.095

Ajji, Z., Maarouf, M., Khattab, A., & Ghazal, H. (2020). Synthesis of pH-responsive hydrogel based on PVP grafted with crotonic acid for controlled drug delivery. *Radiation Physics and Chemistry*, *170*, 108612. https://doi.org/10.1016/J.RADPHYSCHEM.2019.108612

Anju, S., Prajitha, N., Sukanya, V. S., & Mohanan, P. V. (2020). Complicity of degradable polymers in health-care applications. *Materials Today Chemistry*, *16*, 100236. https://doi.org/10.1016/J.MTCHEM.2019.100236

Ashton, P., Crooks, P., Cynkowski, T., Cynkowska, G., & Guo, H. (2000). Means to Achieve Sustained Release of Synergistic Drugs by Conjugation. *Ophthalmology and Visual Science Faculty Patents*. https://uknowledge.uky.edu/ophthalmology_patents/16

Ata, S., Rasool, A., Islam, A., Bibi, I., Rizwan, M., Azeem, M. K., Qureshi, A. ur R., & Iqbal, M. (2020). Loading of Cefixime to pH sensitive chitosan based hydrogel and investigation of controlled release kinetics. *International Journal of Biological Macromolecules*, *155*, 1236–1244. https://doi.org/10.1016/J.IJBIOMAC.2019.11.091

Baghaie, S., Khorasani, M. T., Zarrabi, A., & Moshtaghian, J. (2017). Wound healing properties of PVA/starch/chitosan hydrogel membranes with nano Zinc oxide as antibacterial wound dressing material. *Journal of Biomaterials Science. Polymer Edition*, *28*(18), 2220–2241. https://doi.org/10.1080/09205063.2017.1390383

Bahrami S.B., Kordestani, S.S., Mirzadeh H. & Mansoori P. (2003). *Poly(vinyl alcohol) - Chitosan blends: Preparation, mechanical and physical properties | Request PDF*. Iranian Polymer Journal. https://www.researchgate.net/publication/280017383_Polyvinyl_alcohol_-_Chitosan_blends_Preparation_mechanical_and_physical_properties

Bai, X., Liu, F., Liu, Y., Li, C., Wang, S., Zhou, H., Wang, W., Zhu, H., Winkler, D. A., & Yan, B. (2017). Toward a systematic exploration of nano-bio interactions. *Toxicology and Applied Pharmacology*, *323*, 66–73. https://doi.org/10.1016/J.TAAP.2017.03.011

Baker, M. I., Walsh, S. P., Schwartz, Z., & Boyan, B. D. (2012). A review of polyvinyl alcohol and its uses in cartilage and orthopedic applications. *Journal of Biomedical Materials Research Part B: Applied Biomaterials*, *100B*(5), 1451–1457. https://doi.org/10.1002/JBM.B.32694

Battig, M. R., Soontornworajit, B., & Wang, Y. (2012). Programmable release of multiple protein drugs from aptamer-functionalized hydrogels via nucleic acid hybridization. *Journal of the American Chemical Society*, *134*(30), 12410–12413. https://doi.org/10.1021/JA305238A/SUPPL_FILE/JA305238A_SI_001.PDF

Bhattarai, R. S., Bachu, R. D., Boddu, S. H. S., & Bhaduri, S. (2018). Biomedical Applications of Electrospun Nanofibers: Drug and Nanoparticle Delivery.

*Pharmaceutics 2019, Vol. 11, Page 5*, *11*(1), 5. https://doi.org/10.3390/PHARMACEUTICS11010005

Bockuviene, A., & Sereikaite, J. (2019). Preparation and characterisation of novel water-soluble β-carotene-chitooligosaccharides complexes. *Carbohydrate Polymers*, *225*. https://doi.org/10.1016/J.CARBPOL.2019.115226

Böker, A., Predoi, D., El, R., Billah, K., Ayouch, I., Abdellaoui, Y., Kassab, Z., Khan, A., Agunaou, M., Soufiane, A., Otero, M., & Jeon, B.-H. (2023). A Novel Chitosan/Nano-Hydroxyapatite Composite for the Adsorptive Removal of Cd(II) from Aqueous Solution. *Polymers 2023, Vol. 15, Page 1524*, *15*(6), 1524. https://doi.org/10.3390/POLYM15061524

Boudemagh, D., Venturini, P., Fleutot, S., & Cleymand, F. (2019). Elaboration of hydroxyapatite nanoparticles and chitosan/hydroxyapatite composites: a present status. *Polymer Bulletin*, *76*(5), 2621–2653. https://doi.org/10.1007/S00289-018-2483-Y

Brannon-Peppas, L. (1995). Recent advances on the use of biodegradable microparticles and nanoparticles in controlled drug delivery. *International Journal of Pharmaceutics*, *116*(1), 1–9. https://doi.org/10.1016/0378-5173(94)00324-X

Chung, Y. C., & Chen, C. Y. (2008). Antibacterial characteristics and activity of acid-soluble chitosan. *Bioresource Technology*, *99*(8), 2806–2814. https://doi.org/10.1016/J.BIORTECH.2007.06.044

Colombo, P. (1993). Swelling-controlled release in hydrogel matrices for oral route. *Advanced Drug Delivery Reviews*, *11*(1–2), 37–57. https://doi.org/10.1016/0169-409X(93)90026-Z

Cong, Z., Shi, Y., Wang, Y., Wang, Y., Niu, J., Chen, N., & Xue, H. (2018). A novel controlled drug delivery system based on alginate hydrogel/chitosan micelle composites. *International Journal of Biological Macromolecules*, *107*(Pt A), 855–864. https://doi.org/10.1016/J.IJBIOMAC.2017.09.065

Contreras-Torres, F. F., Rodríguez-Galván, A., Guerrero-Beltrán, C. E., Martínez-Lorán, E., Vázquez-Garza, E., Ornelas-Soto, N., & García-Rivas, G. (2017). Differential cytotoxicity and internalization of graphene family nanomaterials in myocardial cells. *Materials Science and Engineering: C*, *73*, 633–642. https://doi.org/10.1016/J.MSEC.2016.12.080

Dasgupta, S., Bandyopadhyay, A., & Bose, S. (2009). Reverse micelle-mediated synthesis of calcium phosphate nanocarriers for controlled release of bovine serum albumin. *Acta Biomaterialia*, *5*(8), 3112–3121. https://doi.org/10.1016/J.ACTBIO.2009.04.031

De Campos, A. M., Sánchez, A., & Alonso, M. J. (2001). Chitosan nanoparticles: a new vehicle for the improvement of the delivery of drugs to the ocular surface. Application to cyclosporin A. *International Journal of Pharmaceutics*, *224*(1–2), 159–168. https://doi.org/10.1016/S0378-5173(01)00760-8

De Lima, G. G., De Lima, D. W. F., De Oliveira, M. J. A., Lugaõ, A. B., Alcântara, M. T. S., Devine, D. M., & De Sá, M. J. C. (2018). Synthesis and in Vivo Behavior of PVP/CMC/Agar Hydrogel Membranes Impregnated with Silver Nanoparticles for Wound Healing Applications. *ACS Applied Bio Materials*, *1*(6), 1842–1852. https://doi.org/10.1021/ACSABM.8B00369

Deng, L., Li, Y., Zhang, A., & Zhang, H. (2020). Characterization and physical properties of electrospun gelatin nanofibrous films by incorporation of nano-hydroxyapatite. *Food Hydrocolloids*, *103*. https://doi.org/10.1016/j.foodhyd.2019.105640

Diaz del Consuelo, I., Falson, F., Guy, R. H., & Jacques, Y. (2007). Ex vivo evaluation of bioadhesive films for buccal delivery of fentanyl. *Journal of Controlled Release*, *122*(2), 135–140. https://doi.org/10.1016/J.JCONREL.2007.05.017

Dorozhkin, S. V. (2009). Calcium Orthophosphates in Nature, Biology and Medicine. *Materials 2009, Vol. 2, Pages 399-498*, *2*(2), 399–498. https://doi.org/10.3390/MA2020399

Elashmawi, I. S., & Elsayed, N. H. (2020). The role of gold nanoparticles in the structural and electrical properties of Cs/PVP blend. *Polymer Bulletin*, *77*(2), 949–962. https://doi.org/10.1007/S00289-019-02786-Z

Elbasuney, S. (2020). Green Synthesis of Hydroxyapatite Nanoparticles with Controlled Morphologies and Surface Properties Toward Biomedical Applications. *Journal of Inorganic and Organometallic Polymers and Materials*, *30*(3), 899–906. https://doi.org/10.1007/S10904-019-01247-4/METRICS

Eskitoros-Togay, M., Bulbul, Y. E., & Dilsiz, N. (2020). Combination of nano-hydroxyapatite and curcumin in a biopolymer blend matrix: Characteristics and drug release performance of fibrous composite material systems. *International Journal of Pharmaceutics*, *590*. https://doi.org/10.1016/j.ijpharm.2020.119933

Eslami, H., Solati-Hashjin, M., & Tahriri, M. (2009). The comparison of powder characteristics and physicochemical, mechanical and biological properties between nanostructure ceramics of hydroxyapatite and fluoridated hydroxyapatite. *Materials Science and Engineering: C*, *29*(4), 1387–1398. https://doi.org/10.1016/J.MSEC.2008.10.033

Fatema, U. K., Rahman, M. M., Islam, M. R., Mollah, M. Y. A., & Susan, M. A. B. H. (2018). Silver/poly(vinyl alcohol) nanocomposite film prepared using water in oil microemulsion for antibacterial applications. *Journal of Colloid and Interface Science*, *514*, 648–655. https://doi.org/10.1016/J.JCIS.2017.12.084

Fathi, M. H., Hanifi, A., & Mortazavi, V. (2008). Preparation and bioactivity evaluation of bone-like hydroxyapatite nanopowder. *Journal of Materials Processing Technology*, *202*(1–3), 536–542. https://doi.org/10.1016/J.JMATPROTEC.2007.10.004

Fogaça, R., & Catalani, L. H. (2012). PVP Hydrogel Membranes Produced by Electrospinning for Protein Release Devices. *Http://Dx.Doi.Org/10.1080/1539445X.2011.580411*, *11*(1), 61–68. https://doi.org/10.1080/1539445X.2011.580411

Folttmann, H. & Anisul, Q. (2008). *Polyvinylpyrrolidone (PVP) - One of the most widely used excipients in pharmaceuticals: An overview | Request PDF*. https://www.researchgate.net/publication/284634349_Polyvinylpyrrolidone_PVP_-_One_of_the_most_widely_used_excipients_in_pharmaceuticals_An_overview

Galindo, T. G. P., Chai, Y., & Tagaya, M. (2019). Hydroxyapatite nanoparticle coating on polymer for constructing effective biointeractive interfaces. *Journal of Nanomaterials*, *2019*. https://doi.org/10.1155/2019/6495239

Gao, H., He, J., Yang, R., & Yang, L. (2010). Characteristic rheological features of high concentration PVA solutions in water with different degrees of polymerization. *Journal of Applied Polymer Science*, *116*(5), 2734–2741. https://doi.org/10.1002/APP.31900

George, D., Maheswari, P. U., & Begum, K. M. M. S. (2019). Synergic formulation of onion peel quercetin loaded chitosan-cellulose hydrogel with green zinc oxide nanoparticles towards controlled release, biocompatibility, antimicrobial and

anticancer activity. *International Journal of Biological Macromolecules*, *132*, 784–794. https://doi.org/10.1016/J.IJBIOMAC.2019.04.008

Ghauri, Z. H., Islam, A., Qadir, M. A., Gull, N., Haider, B., Khan, R. U., & Riaz, T. (2021). Development and evaluation of pH-sensitive biodegradable ternary blended hydrogel films (chitosan/guar gum/PVP) for drug delivery application. *Scientific Reports*, *11*(1). https://doi.org/10.1038/s41598-021-00452-x

Giang Phan, V. H., Duong, H. T. T., Thambi, T., Nguyen, T. L., Turabee, M. H., Yin, Y., Kim, S. H., Kim, J., Jeong, J. H., & Lee, D. S. (2019). Modularly engineered injectable hybrid hydrogels based on protein-polymer network as potent immunologic adjuvant in vivo. *Biomaterials*, *195*, 100–110. https://doi.org/10.1016/J.BIOMATERIALS.2018.12.034

Gierszewska-Drużyńska, M., & Ostrowska-Czubenko, J. (2011). *(PDF) Influence of crosslinking process conditions on molecular and supermolecular structure of chitosan hydrogel membrane*. https://www.researchgate.net/publication/285466475_Influence_of_crosslinking_process_conditions_on_molecular_and_supermolecular_structure_of_chitosan_hydrogel_membrane

Ginebra, M. P., Canal, C., Espanol, M., Pastorino, D., & Montufar, E. B. (2012). Calcium phosphate cements as drug delivery materials. *Advanced Drug Delivery Reviews*, *64*(12), 1090–1110. https://doi.org/10.1016/J.ADDR.2012.01.008

Giri, T. K., Thakur, A., Alexander, A., Ajazuddin, Badwaik, H., & Tripathi, D. K. (2012). Modified chitosan hydrogels as drug delivery and tissue engineering systems: present status and applications. *Acta Pharmaceutica Sinica B*, *2*(5), 439–449. https://doi.org/10.1016/J.APSB.2012.07.004

Grande, R., Pessan, L. A., & Carvalho, A. J. F. (2018). Thermoplastic blends of chitosan: A method for the preparation of high thermally stable blends with polyesters. *Carbohydrate Polymers*, *191*, 44–52. https://doi.org/10.1016/J.CARBPOL.2018.02.087

Guerrero-Beltrán, C. E., Bernal-Ramírez, J., Lozano, O., Oropeza-Almazán, Y., Castillo, E. C., Garza, J. R., García, N., Vela, J., García-García, A., Ortega, E., Torre-Amione, G., Ornelas-Soto, N., & García-Rivas, G. (2017). Silica nanoparticles induce cardiotoxicity interfering with energetic status and Ca2+ handling in adult rat cardiomyocytes. *American Journal of Physiology - Heart and Circulatory Physiology*, *312*(4), H645–H661. https://doi.org/10.1152/AJPHEART.00564.2016/SUPPL_FILE/SUPPLEMENTAL

Gupta, P., Vermani, K., & Garg, S. (2002). Hydrogels: from controlled release to pH-responsive drug delivery. *Drug Discovery Today*, *7*(10), 569–579. https://doi.org/10.1016/S1359-6446(02)02255-9

Gupta, R., & Mukherjee, B. (2003). Development and In Vitro Evaluation of Diltiazem Hydrochloride Transdermal Patches Based on Povidone–EthylCellulose Matrices. *Http://Dx.Doi.Org/10.1081/DDC-120016678*, *29*(1), 1–7. https://doi.org/10.1081/DDC-120016678

Hafeez, S., Islam, A., Gull, N., Ali, A., Khan, S. M., Zia, S., Anwar, K., Khan, S. U., & Jamil, T. (2018). γ-Irradiated chitosan based injectable hydrogels for controlled release of drug (Montelukast sodium). *International Journal of Biological Macromolecules*, *114*, 890–897. https://doi.org/10.1016/J.IJBIOMAC.2018.02.107

Hassan, C. M., & Peppas, N. A. (2000). Structure and applications of poly(vinyl alcohol) hydrogels produced by conventional crosslinking or by freezing/thawing methods.

*Advances in Polymer Science*, *153*, 37–65. https://doi.org/10.1007/3-540-46414-X_2/COVER

Hatefi, A., & Amsden, B. (2002). Biodegradable injectable in situ forming drug delivery systems. *Journal of Controlled Release*, *80*(1–3), 9–28. https://doi.org/10.1016/S0168-3659(02)00008-1

Hecold, M., Buczkowska, R., Mucha, A., … J. G.-J. of, & 2017, undefined. (2017). The effect of PEI and PVP-stabilized gold nanoparticles on equine platelets activation: Potential application in equine regenerative medicine. *Hindawi.Com*. https://www.hindawi.com/journals/jnm/2017/8706921/

He, P., Davis, S. S., & Illum, L. (1998). In vitro evaluation of the mucoadhesive properties of chitosan microspheres. *International Journal of Pharmaceutics*, *166*(1), 75–88. https://doi.org/10.1016/S0378-5173(98)00027-1

Hu, M., Li, C., Li, X., Zhou, M., Sun, J., Sheng, F., Shi, S., & Lu, L. (2018). Zinc oxide/silver bimetallic nanoencapsulated in PVP/PCL nanofibres for improved antibacterial activity. *Artificial Cells, Nanomedicine and Biotechnology*, *46*(6), 1248–1257. https://doi.org/10.1080/21691401.2017.1366339

Iqbal, D. N., Ehtisham-ul-Haque, S., Ahmad, S., Arif, K., Hussain, E. A., Iqbal, M., Alshawwa, S. Z., Abbas, M., Amjed, N., & Nazir, A. (2021). Enhanced antibacterial activity of chitosan, guar gum and polyvinyl alcohol blend matrix loaded with amoxicillin and doxycycline hyclate drugs. *Arabian Journal of Chemistry*, *14*(6). https://doi.org/10.1016/j.arabjc.2021.103156

Iqbal, D. N., Tariq, M., Khan, S. M., Gull, N., Sagar Iqbal, S., Aziz, A., Nazir, A., & Iqbal, M. (2020). Synthesis and characterization of chitosan and guar gum based ternary blends with polyvinyl alcohol. *International Journal of Biological Macromolecules*, *143*, 546–554. https://doi.org/10.1016/j.ijbiomac.2019.12.043

Jaganathan, S. K., Mani, M. P., Khudzari, A. Z. M., Ismail, A. F., Ayyar, M., & Rathanasamy, R. (2019). Enriched physicochemical and blood-compatible properties of nanofibrous polyurethane patch engrafted with juniper oil and titanium dioxide for cardiac tissue engineering. *International Journal of Polymer Analysis and Characterization*, *24*(8), 696–708. https://doi.org/10.1080/1023666X.2019.1662590

Jaganathan, S. K., Prasath Mani, M., Ayyar, M., & Rathanasamy, R. (2019). Biomimetic electrospun polyurethane matrix composites with tailor made properties for bone tissue engineering scaffolds. *Polymer Testing*, *78*. https://doi.org/10.1016/j.polymertesting.2019.105955

Jamaledin, R., Makvandi, P., Yiu, C. K. Y., Agarwal, T., Vecchione, R., Sun, W., Maiti, T. K., Tay, F. R., & Netti, P. A. (2020). Engineered Microneedle Patches for Controlled Release of Active Compounds: Recent Advances in Release Profile Tuning. *Advanced Therapeutics*, *3*(12), 2000171. https://doi.org/10.1002/ADTP.202000171

Janugade, B., Patil, S., Patil, S., Res, P. L.-J. P., & 2009, undefined. (n.d.). Effect of PVP concentration on lag time of press-coated Montelukast sodium tablet. *Researchgate.Net*. Retrieved March 17, 2023, from https://www.researchgate.net/profile/Sachinkumar-Patil-2/publication/265687658_Effect_of_PVP_concentration_on_lag_time_of_press-coated_Montelukast_sodium_tablet/links/541930940cf2218008bf5377/Effect-of-PVP-concentration-on-lag-time-of-press-coated-Montelukast-sodium-tablet.pdf

Jipa, I. M., Stoica, A., Stroescu, M., Dobre, L. M., Dobre, T., Jinga, S., & Tardei, C. (2012). Potassium sorbate release from poly(vinyl alcohol)-bacterial cellulose

films. *Chemical Papers*, *66*(2), 138–143. https://doi.org/10.2478/s11696-011-0068-4

Johns, J., & Rao, V. (2008). Characterization of natural rubber latex/chitosan blends. *International Journal of Polymer Analysis and Characterization*, *13*(4), 280–291. https://doi.org/10.1080/10236660802190104

Jooybar, E., Tajsoleiman, T., & Abdekhodaie, M. J. (2021). Theoretical study of diffusional release of a dispersed solute from a hollow cylindrical polymeric matrix. *Scientia Iranica*, *28*(3), 1428–1435. https://doi.org/10.24200/SCI.2021.53502.3271

Jung, Y., & Kim, Y. M. (2010). What should be considered on design of a colon-specific prodrug? *Expert Opinion on Drug Delivery*, *7*(2), 245–258. https://doi.org/10.1517/17425240903490401

Kadhim, KadhimJ., Agool, IbrahimR., & Hashim, A. (2016). Synthesis of (PVA-PEG-PVP-TiO 2 ) Nanocomposites for Antibacterial Application . *Materials Focus*, *5*(5), 436–439. https://doi.org/10.1166/MAT.2016.1371

Karavas, E., Georgarakis, E., & Bikiaris, D. (2006). Application of PVP/HPMC miscible blends with enhanced mucoadhesive properties for adjusting drug release in predictable pulsatile chronotherapeutics. *European Journal of Pharmaceutics and Biopharmaceutics*, *64*(1), 115–126. https://doi.org/10.1016/J.EJPB.2005.12.013

Kenawy, E. R., El-Newehy, M. H., & Al-Deyab, S. S. (2010). Controlled release of atenolol from freeze/thawed poly(vinyl alcohol) hydrogel. *Journal of Saudi Chemical Society*, *14*(2), 237–240. https://doi.org/10.1016/J.JSCS.2010.02.014

Kester, M., Heakal, Y., Fox, T., Sharma, A., Robertson, G. P., Morgan, T. T., Altinoğlu, E. I., Tabaković, A., Parette, M. R., Rouse, S. M., Ruiz-Velasco, V., & Adair, J. H. (2008). Calcium phosphate nanocomposite particles for in vitro imaging and encapsulated chemotherapeutic drug delivery to cancer Cells. *Nano Letters*, *8*(12), 4116–4121. https://doi.org/10.1021/NL802098G/SUPPL_FILE/NL802098G_SI_001.PDF

Khalid, H., & Chaudhry, A. A. (2020). Basics of hydroxyapatite—structure, synthesis, properties, and clinical applications. *Handbook of Ionic Substituted Hydroxyapatites*, 85–115. https://doi.org/10.1016/B978-0-08-102834-6.00004-5

Kucharska, M., Walenko, K., Lewandowska-Szumieł, M., Brynk, T., Jaroszewicz, J., & Ciach, T. (2015). Chitosan and composite microsphere-based scaffold for bone tissue engineering: evaluation of tricalcium phosphate content influence on physical and biological properties. *Journal of Materials Science. Materials in Medicine*, *26*(3). https://doi.org/10.1007/S10856-015-5464-9

Kurakula, M., & Rao, G. S. N. K. (2020). Pharmaceutical assessment of polyvinylpyrrolidone (PVP): As excipient from conventional to controlled delivery systems with a spotlight on COVID-19 inhibition. *Journal of Drug Delivery Science and Technology*, *60*, 102046. https://doi.org/10.1016/J.JDDST.2020.102046

Lafayette, W. (2016). *Drug Delivery: Fundamentals & Applications, 2nd Edition*. https://www.routledge.com/Drug-Delivery-Fundamentals-and-Applications-Second-Edition/Hillery-Park/p/book/9781482217711

Langer, R. (1990). New methods of drug delivery. *Science*, *249*(4976), 1527–1533. https://doi.org/10.1126/SCIENCE.2218494

Langer, R. (2007). INVITED REVIEW POLYMERIC DELIVERY SYSTEMS FOR CONTROLLED DRUG RELEASE.

*Http://Dx.Doi.Org/10.1080/00986448008912519*, *6*(1–3), 1–48. https://doi.org/10.1080/00986448008912519

Lee, B. K., Yun, Y. H., & Park, K. (2015). Smart Nanoparticles for Drug Delivery: Boundaries and Opportunities. *Chemical Engineering Science*, *125*, 158. https://doi.org/10.1016/J.CES.2014.06.042

Lee, P., and, J. L.-O. controlled release formulation design, & 2010, undefined. (2010). Evolution of oral controlled release dosage forms. *Books.Google.Com*. https://books.google.com/books?hl=en&lr=&id=01kWYaIg77QC&oi=fnd&pg=PA21&dq=.I.+Lee,+J.X.+Li,+Evolution+of+oral+controlled+release+dosage+forms,+in:+H.+Wen,+K.+Park+(Eds.)+Oral+Controlled+Release+Formulation+Design+and+Drug+Delivery,+John+Wiley+%26+Sons,+Inc.,+Hoboken,+NJ,+2010,+pp.+21-31.&ots=h2qWY5elUA&sig=YFtt52D-mUXCimq_mhG4P5c87Vc

Lee, W. H., Loo, C. Y., & Rohanizadeh, R. (2014). A review of chemical surface modification of bioceramics: Effects on protein adsorption and cellular response. *Colloids and Surfaces B: Biointerfaces*, *122*, 823–834. https://doi.org/10.1016/J.COLSURFB.2014.07.029

Lehr, C. M., Bouwstra, J. A., Schacht, E. H., & Junginger, H. E. (1992). In vitro evaluation of mucoadhesive properties of chitosan and some other natural polymers. *International Journal of Pharmaceutics*, *78*(1–3), 43–48. https://doi.org/10.1016/0378-5173(92)90353-4

Li, J., & Mooney, D. J. (2016). Designing hydrogels for controlled drug delivery. *Nature Reviews Materials 2016 1:12*, *1*(12), 1–17. https://doi.org/10.1038/natrevmats.2016.71

Lim, S. H., & Hudson, S. M. (2004). Synthesis and antimicrobial activity of a water-soluble chitosan derivative with a fiber-reactive group. *Carbohydrate Research*, *339*(2), 313–319. https://doi.org/10.1016/j.carres.2003.10.024

Liu, J., Lin, S., Li, L., & Liu, E. (2005). Release of theophylline from polymer blend hydrogels. *International Journal of Pharmaceutics*, *298*(1), 117–125. https://doi.org/10.1016/J.IJPHARM.2005.04.006

Li, X., Zhang, F., Sun, X., Hu, Y., Song, A., & Hao, J. (2018). Hydrogels formed by L-histidine derivatives with highly selective release for charged dyes. *Chinese Chemical Letters*, *29*(8), 1219–1222. https://doi.org/10.1016/J.CCLET.2017.12.024

Luo, Q., Shan, Y., Zuo, X., & Liu, J. (2018). Anisotropic tough poly(vinyl alcohol)/graphene oxide nanocomposite hydrogels for potential biomedical applications. *RSC Advances*, *8*(24), 13284–13291. https://doi.org/10.1039/C8RA00340H

Mahato, K. K., Sabbarwal, S., Misra, N., & Kumar, M. (2020). Fabrication of polyvinyl alcohol/chitosan oligosaccharide hydrogel: physicochemical characterizations and in vitro drug release study. *International Journal of Polymer Analysis and Characterization*, 353–361. https://doi.org/10.1080/1023666X.2020.1789382

Mahdavinia, G. R., Soleymani, M., Etemadi, H., Sabzi, M., & Atlasi, Z. (2018). Model protein BSA adsorption onto novel magnetic chitosan/PVA/laponite RD hydrogel nanocomposite beads. *International Journal of Biological Macromolecules*, *107*(PartA), 719–729. https://doi.org/10.1016/J.IJBIOMAC.2017.09.042

Maitra, J., & Shukla, V. K. (2014). Cross-linking in Hydrogels - A Review. *American Journal of Polymer Science*, *4*(2), 25–31. https://doi.org/10.5923/J.AJPS.20140402.01

Marcos Luciano Bruschi. (2015). Strategies to Modify the Drug Release from Pharmaceutical Systems. *Strategies to Modify the Drug Release from Pharmaceutical Systems*, 87–194. http://www.sciencedirect.com/science/article/pii/B9780081000922000060

Martin, L., Wilson, C. G., Koosha, F., Tetley, L., Gray, A. I., Senel, S., & Uchegbu, I. F. (2002). The release of model macromolecules may be controlled by the hydrophobicity of palmitoyl glycol chitosan hydrogels. *Journal of Controlled Release*, *80*(1–3), 87–100. https://doi.org/10.1016/S0168-3659(02)00005-6

Mathiowitz, E. (1999). *Encyclopedia of controlled drug delivery*. 1057. https://www.wiley.com/en-us/Encyclopedia+of+Controlled+Drug+Delivery%2C+2+Volume+Set-p-9780471148289

Matsumoto, T., Okazaki, M., Inoue, M., Yamaguchi, S., Kusunose, T., Toyonaga, T., Hamada, Y., & Takahashi, J. (2004). Hydroxyapatite particles as a controlled release carrier of protein. *Biomaterials*, *25*(17), 3807–3812. https://doi.org/10.1016/J.BIOMATERIALS.2003.10.081

Melo-Silveira, R. F., Fidelis, G. P., Pereira Costa, M. S. S., Telles, C. B. S., Dantas-Santos, N., de Oliveira Elias, S., Ribeiro, V. B., Barth, A. L., Macedo, A. J., Leite, E. L., & Rocha, H. A. O. (2012). In Vitro Antioxidant, Anticoagulant and Antimicrobial Activity and in Inhibition of Cancer Cell Proliferation by Xylan Extracted from Corn Cobs. *International Journal of Molecular Sciences*, *13*(1), 409. https://doi.org/10.3390/IJMS13010409

Mishra, R. K., Datt, M., & Banthia, A. K. (2008). Synthesis and characterization of pectin/pvp hydrogel membranes for drug delivery system. *AAPS PharmSciTech*, *9*(2), 395–403. https://doi.org/10.1208/S12249-008-9048-6/METRICS

Mohabe, V., Akhand, R., Res, A. P.-Bull. Pharm., & 2011, undefined. (n.d.). Preparation and evaluation of captopril transdermal patches. *Researchgate.Net*. Retrieved March 17, 2023, from https://www.researchgate.net/profile/Rachana-Akhand-Giri2/publication/328213985_PREPARATION_AND_EVALUATION_OF_CAPTOPRIL_TRANSDERMAL_PATCHES/links/5bbefc0845851572315edb91/PREPARATION-AND-EVALUATION-OF-CAPTOPRIL-TRANSDERMAL-PATCHES.pdf

Mohamed, R. R., Elella, M. H. A., & Sabaa, M. W. (2017). Cytotoxicity and metal ions removal using antibacterial biodegradable hydrogels based on N-quaternized chitosan/poly(acrylic acid). *International Journal of Biological Macromolecules*, *98*, 302–313. https://doi.org/10.1016/J.IJBIOMAC.2017.01.107

Munir, M. U., Ihsan, A., Sarwar, Y., Bajwa, S. Z., Bano, K., Tehseen, B., Zeb, N., Hussain, I., Ansari, M. T., Saeed, M., Li, J., Iqbal, M. Z., Wu, A., & Khan, W. S. (2018). Hollow mesoporous hydroxyapatite nanostructures; smart nanocarriers with high drug loading and controlled releasing features. *International Journal of Pharmaceutics*, *544*(1), 112–120. https://doi.org/10.1016/J.IJPHARM.2018.04.029

Nho, Y. C., & Park, K. R. (2002). Preparation and properties of PVA/PVP hydrogels containing chitosan by radiation. *Journal of Applied Polymer Science*, *85*(8), 1787–1794. https://doi.org/10.1002/APP.10812

Niu, Y., Yang, T., Ke, R., & Wang, C. (2019). Preparation and characterization of ph-responsive sodium alginate/humic acid/konjac hydrogel for l-ascorbic acid controlled release. *Materials Express*, *9*(6), 563–569. https://doi.org/10.1166/MEX.2019.1537

Ollier, R., Pérez, C. J., & Alvarez, V. (2012). Effect of Relative Humidity on the Mechanical Properties of Micro and Nanocomposites of Polyvinyl Alcohol. *Procedia Materials Science*, *1*, 499–505. https://doi.org/10.1016/J.MSPRO.2012.06.067

Omidian, H., & Park, K. (2008). Swelling agents and devices in oral drug delivery. *Journal of Drug Delivery Science and Technology*, *18*(2), 83–93. https://doi.org/10.1016/S1773-2247(08)50016-5

Ornelas-Soto, N., Rubio-Govea, R., Guerrero-Beltrán, C. E., Vázquez-Garza, E., Bernal-Ramírez, J., García-García, A., Oropeza-Almazán, Y., García-Rivas, G., & Contreras-Torres, F. F. (2017). Enhancing internalization of silica particles in myocardial cells through surface modification. *Materials Science and Engineering: C*, *79*, 831–840. https://doi.org/10.1016/J.MSEC.2017.05.092

Pal, S., Tak, Y. K., & Song, J. M. (2007). Does the antibacterial activity of silver nanoparticles depend on the shape of the nanoparticle? A study of the gram-negative bacterium Escherichia coli. *Applied and Environmental Microbiology*, *73*(6), 1712–1720. https://doi.org/10.1128/AEM.02218-06/ASSET/6C9C03C4-A4A8-46FD-9451-902F4F8671C3/ASSETS/GRAPHIC/ZAM0060775900008.JPEG

Park, K. (2013). Facing the truth about nanotechnology in drug delivery. *ACS Nano*, *7*(9), 7442–7447. https://doi.org/10.1021/NN404501G/ASSET/IMAGES/MEDIUM/NN-2013-04501G_0003.GIF

Park, K. (2014). Controlled drug delivery systems: past forward and future back. *Journal of Controlled Release : Official Journal of the Controlled Release Society*, *190*, 3–8. https://doi.org/10.1016/J.JCONREL.2014.03.054

Park, K. (2016). Drug delivery of the future: Chasing the invisible gorilla. *Journal of Controlled Release*, *240*, 2–8. https://doi.org/10.1016/J.JCONREL.2015.10.048

Peng, X., He, C., Liu, J., & Wang, H. (2016a). Biomimetic jellyfish-like PVA/graphene oxide nanocomposite hydrogels with anisotropic and pH-responsive mechanical properties. *Journal of Materials Science*, *51*(12), 5901–5911. https://doi.org/10.1007/S10853-016-9891-X/FIGURES/8

Peng, X., He, C., Liu, J., & Wang, H. (2016b). Biomimetic jellyfish-like PVA/graphene oxide nanocomposite hydrogels with anisotropic and pH-responsive mechanical properties. *Journal of Materials Science*, *51*(12), 5901–5911. https://doi.org/10.1007/S10853-016-9891-X/FIGURES/8

Peppas, N. A., & Sahlin, J. J. (1996). Hydrogels as mucoadhesive and bioadhesive materials: a review. *Biomaterials*, *17*(16), 1553–1561. https://doi.org/10.1016/0142-9612(95)00307-X

Perioli, L., Ambrogi, V., Angelici, F., Ricci, M., Giovagnoli, S., Capuccella, M., & Rossi, C. (2004). Development of mucoadhesive patches for buccal administration of ibuprofen. *Journal of Controlled Release*, *99*(1), 73–82. https://doi.org/10.1016/J.JCONREL.2004.06.005

Phatai, P., Futalan, C. M., Kamonwannasit, S., & Khemthong, P. (2019). Structural characterization and antibacterial activity of hydroxyapatite synthesized via sol-gel method using glutinous rice as a template. *Journal of Sol-Gel Science and Technology*, *89*(3), 764–775. https://doi.org/10.1007/S10971-018-4910-9/METRICS

Pighinelli, L., & Kucharska, M. (2013). Chitosan–hydroxyapatite composites. *Carbohydrate Polymers*, *93*(1), 256–262. https://doi.org/10.1016/J.CARBPOL.2012.06.004

Prakash, J., Kumar, T. S., Venkataprasanna, K. S., Niranjan, R., Kaushik, M., Samal, D. B., & Venkatasubbu, G. D. (2019a). PVA/alginate/hydroxyapatite films for controlled release of amoxicillin for the treatment of periodontal defects. *Applied Surface Science*, *495*. https://doi.org/10.1016/j.apsusc.2019.143543

Prakash, J., Kumar, T. S., Venkataprasanna, K. S., Niranjan, R., Kaushik, M., Samal, D. B., & Venkatasubbu, G. D. (2019b). PVA/alginate/hydroxyapatite films for controlled release of amoxicillin for the treatment of periodontal defects. *Applied Surface Science*, *495*. https://doi.org/10.1016/j.apsusc.2019.143543

Prakash, J., Kumar, T. S., Venkataprasanna, K. S., Niranjan, R., Kaushik, M., Samal, D. B., & Venkatasubbu, G. D. (2019c). PVA/alginate/hydroxyapatite films for controlled release of amoxicillin for the treatment of periodontal defects. *Applied Surface Science*, *495*. https://doi.org/10.1016/j.apsusc.2019.143543

Priya James, H., John, R., Alex, A., & Anoop, K. R. (2014). Smart polymers for the controlled delivery of drugs - a concise overview. *Acta Pharmaceutica Sinica. B*, *4*(2), 120–127. https://doi.org/10.1016/J.APSB.2014.02.005

Qi, X., Liu, R., Chen, M., Li, Z., Qin, T., Qian, Y., Zhao, S., Liu, M., Zeng, Q., & Shen, J. (2019). Removal of copper ions from water using polysaccharide-constructed hydrogels. *Carbohydrate Polymers*, *209*, 101–110. https://doi.org/10.1016/j.carbpol.2019.01.015

Rajiv Gandhi, M., Kousalya, G. N., & Meenakshi, S. (2011). Removal of copper(II) using chitin/chitosan nano-hydroxyapatite composite. *International Journal of Biological Macromolecules*, *48*(1), 119–124. https://doi.org/10.1016/J.IJBIOMAC.2010.10.009

Ramalingam, V., Varunkumar, K., Ravikumar, V., & Rajaram, R. (2018). Target delivery of doxorubicin tethered with PVP stabilized gold nanoparticles for effective treatment of lung cancer. *Scientific Reports*, *8*(1). https://doi.org/10.1038/S41598-018-22172-5

Raneque, M. R., Nucleus, A. R. R.-, & 2013, undefined. (n.d.). Hydrogel wound dressing preparation at laboratory scale by using electron beam and gamma radiation. *Search.Ebscohost.Com*. Retrieved March 17, 2023, from https://search.ebscohost.com/login.aspx?direct=true&profile=ehost&scope=site&authtype=crawler&jrnl=0864084X&AN=109102056&h=awv2caAz5bBb5lisC5w8ZD0uv9euC8LyTTCwbkRXsGr0lg0BtxGpqXgYMe0JJyeCj8TzGQId9ALervEIAaw32w%3D%3D&crl=c

Rasool, A., Ata, S., & Islam, A. (2019). Stimuli responsive biopolymer (chitosan) based blend hydrogels for wound healing application. *Carbohydrate Polymers*, *203*, 423–429. https://doi.org/10.1016/J.CARBPOL.2018.09.083

Rasool, A., Ata, S., Islam, A., & Khan, R. U. (2019). Fabrication of novel carrageenan based stimuli responsive injectable hydrogels for controlled release of cephradine. *RSC Advances*, *9*(22), 12282–12290. https://doi.org/10.1039/C9RA02130B

Ravi Kumar, M. N. V. (2000). A review of chitin and chitosan applications. *Reactive and Functional Polymers*, *46*(1), 1–27. https://doi.org/10.1016/S1381-5148(00)00038-9

Rinaudo, M. (2006). Chitin and chitosan: Properties and applications. *Progress in Polymer Science*, *31*(7), 603–632. https://doi.org/10.1016/J.PROGPOLYMSCI.2006.06.001

Risbud, M. V., Hardikar, A. A., Bhat, S. V., & Bhonde, R. R. (2000). pH-sensitive freeze-dried chitosan–polyvinyl pyrrolidone hydrogels as controlled release system for antibiotic delivery. *Journal of Controlled Release*, *68*(1), 23–30. https://doi.org/10.1016/S0168-3659(00)00208-X

Rivera-Hernández, G., Antunes-Ricardo, M., Martínez-Morales, P., & Sánchez, M. L. (2021). Polyvinyl alcohol based-drug delivery systems for cancer treatment. In *International Journal of Pharmaceutics* (Vol. 600). Elsevier B.V. https://doi.org/10.1016/j.ijpharm.2021.120478

Rizwan, M., Yahya, R., Hassan, A., Yar, M., Azzahari, A. D., Selvanathan, V., Sonsudin, F., & Abouloula, C. N. (2017). pH Sensitive Hydrogels in Drug Delivery: Brief History, Properties, Swelling, and Release Mechanism, Material Selection and Applications. *Polymers*, *9*(4). https://doi.org/10.3390/POLYM9040137

Rolim, W. R., Pieretti, J. C., Renó, D. L. S., Lima, B. A., Nascimento, M. H. M., Ambrosio, F. N., Lombello, C. B., Brocchi, M., De Souza, A. C. S., & Seabra, A. B. (2019). Antimicrobial Activity and Cytotoxicity to Tumor Cells of Nitric Oxide Donor and Silver Nanoparticles Containing PVA/PEG Films for Topical Applications. *ACS Applied Materials and Interfaces*. https://doi.org/10.1021/ACSAMI.8B19021/SUPPL_FILE/AM8B19021_SI_001.PDF

Rosen, H. B., Chang, J., Wnek, G. E., Linhardt, R. J., & Langer, R. (1983). Bioerodible polyanhydrides for controlled drug delivery. *Biomaterials*, *4*(2), 131–133. https://doi.org/10.1016/0142-9612(83)90054-6

Rose, P. A., Praseetha, P. K., Bhagat, M., Alexander, P., Abdeen, S., & Chavali, M. (2013). Drug embedded PVP coated magnetic nanoparticles for targeted killing of breast cancer cells. *Technology in Cancer Research and Treatment*, *12*(5), 463–472. https://doi.org/10.7785/TCRT.2012.500333

Rossi, A., Fortuna, M. C., Caro, G., Pranteda, G., Garelli, V., Pompili, U., & Carlesimo, M. (2017). Chemotherapy-induced alopecia management: Clinical experience and practical advice. *Journal of Cosmetic Dermatology*, *16*(4), 537–541. https://doi.org/10.1111/JOCD.12308

Rouahi, M., Champion, E., Gallet, O., Jada, A., & Anselme, K. (2006). Physico-chemical characteristics and protein adsorption potential of hydroxyapatite particles: Influence on in vitro biocompatibility of ceramics after sintering. *Colloids and Surfaces B: Biointerfaces*, *47*(1), 10–19. https://doi.org/10.1016/J.COLSURFB.2005.11.015

Rowe, R. C., Sheskey, P. J., Cook, W. G., Fenton, M. E., & American Pharmacists Association. (2013). *Handbook of pharmaceutical excipients*. 1033.

Sacco, P., Paoletti, S., Cok, M., Asaro, F., Abrami, M., Grassi, M., & Donati, I. (2016). Insight into the ionotropic gelation of chitosan using tripolyphosphate and pyrophosphate as cross-linkers. *International Journal of Biological Macromolecules*, *92*, 476–483. https://doi.org/10.1016/J.IJBIOMAC.2016.07.056

Sadashivaiah, R., … B. D.-A. J. of, & 2008, undefined. (n.d.). Design and in vitro evaluation of haloperidol lactate transdermal patches containing ethyl cellulose-povidone as film formers. *Asiapharmaceutics.Info*. Retrieved March 17, 2023, from http://www.asiapharmaceutics.info/index.php/ajp/article/view/173

Sánchez-Aguinagalde, O., Lejardi, A., Meaurio, E., Hernández, R., Mijangos, C., & Sarasua, J. R. (2021). Novel Hydrogels of Chitosan and Poly(vinyl alcohol) Reinforced with Inorganic Particles of Bioactive Glass. *Polymers*, *13*(5), 1–15. https://doi.org/10.3390/POLYM13050691

Santos, R. M. (2006). Physicochemical Principles of Pharmacy. *American Journal of Pharmaceutical Education*, *70*(5). /pmc/articles/PMC1637007/

Saxena, A., Mozumdar, S., & Johri, A. K. (2006). Ultra-low sized cross-linked polyvinylpyrrolidone nanoparticles as non-viral vectors for in vivo gene delivery. *Biomaterials*, *27*(32), 5596–5602. https://doi.org/10.1016/J.BIOMATERIALS.2006.06.029

Sebastiammal, S., Lesly Fathima, A. S., Devanesan, S., AlSalhi, M. S., Henry, J., Govindarajan, M., & Vaseeharan, B. (2020). Curcumin-encased hydroxyapatite nanoparticles as novel biomaterials for antimicrobial, antioxidant and anticancer applications: A perspective of nano-based drug delivery. *Journal of Drug Delivery Science and Technology*, *57*, 101752. https://doi.org/10.1016/J.JDDST.2020.101752

Selvakumar, M., Srivastava, P., Pawar, H. S., Francis, N. K., Das, B., Sathishkumar, G., Subramanian, B., Jaganathan, S. K., George, G., Anandhan, S., Dhara, S., Nando, G. B., & Chattopadhyay, S. (2016). On-Demand Guided Bone Regeneration with Microbial Protection of Ornamented SPU Scaffold with Bismuth-Doped Single Crystalline Hydroxyapatite: Augmentation and Cartilage Formation. *ACS Applied Materials and Interfaces*, *8*(6), 4086–4100. https://doi.org/10.1021/ACSAMI.5B11723/SUPPL_FILE/AM5B11723_SI_001.PDF

Shakir, M., Jolly, R., Khan, M. S., Iram, N. e., & Khan, H. M. (2015). Nano-hydroxyapatite/chitosan-starch nanocomposite as a novel bone construct: Synthesis and in vitro studies. *International Journal of Biological Macromolecules*, *80*, 282–292. https://doi.org/10.1016/J.IJBIOMAC.2015.05.009

Sheu, S. J., Chou, L. C., Bee, Y. S., Chen, J. F., Lin, H. C., Lin, P. R., Lam, H. C., & Tai, M. H. (2005). Suppression of choroidal neovascularization by intramuscular polymer-based gene delivery of vasostatin. *Experimental Eye Research*, *81*(6), 673–679. https://doi.org/10.1016/J.EXER.2005.04.005

Shi, Q., Liu, H., Tang, D., Li, Y., Li, X. J., & Xu, F. (2019). Bioactuators based on stimulus-responsive hydrogels and their emerging biomedical applications. *NPG Asia Materials 2019 11:1*, *11*(1), 1–21. https://doi.org/10.1038/s41427-019-0165-3

Siegel, R. A. (2000). Theoretical analysis of inward hemispheric release above and below drug solubility. *Journal of Controlled Release : Official Journal of the Controlled Release Society*, *69*(1), 109–126. https://doi.org/10.1016/S0168-3659(00)00292-3

Siegel, R. A., & Rathbone, M. J. (2012). Overview of controlled release mechanisms. *Fundamentals and Applications of Controlled Release Drug Delivery*, 19–43. https://doi.org/10.1007/978-1-4614-0881-9_2

Singh, P., Carrier, A., Chen, Y., Lin, S., Wang, J., Cui, S., & Zhang, X. (2019). Polymeric microneedles for controlled transdermal drug delivery. *Journal of Controlled Release : Official Journal of the Controlled Release Society*, *315*, 97–113. https://doi.org/10.1016/J.JCONREL.2019.10.022

Sizílio, R. H., Galvão, J. G., Trindade, G. G. G., Pina, L. T. S., Andrade, L. N., Gonsalves, J. K. M. C., Lira, A. A. M., Chaud, M. V., Alves, T. F. R., Arguelho, M. L. P. M., & Nunes, R. S. (2018). Chitosan/pvp-based mucoadhesive membranes as a promising delivery system of betamethasone-17-valerate for aphthous stomatitis. *Carbohydrate Polymers*, *190*, 339–345. https://doi.org/10.1016/J.CARBPOL.2018.02.079

Song, C., Yu, H., Zhang, M., Yang, Y., & Zhang, G. (2013). Physicochemical properties and antioxidant activity of chitosan from the blowfly Chrysomya megacephala

larvae. *International Journal of Biological Macromolecules*, *60*, 347–354. https://doi.org/10.1016/J.IJBIOMAC.2013.05.039

Son, G. H., Lee, B. J., & Cho, C. W. (2017). Mechanisms of drug release from advanced drug formulations such as polymeric-based drug-delivery systems and lipid nanoparticles. *Journal of Pharmaceutical Investigation*, *47*(4), 287–296. https://doi.org/10.1007/S40005-017-0320-1/FIGURES/7

Song, S. I., & Kim, B. C. (2004). Characteristic rheological features of PVA solutions in water-containing solvents with different hydration states. *Polymer*, *45*(7), 2381–2386. https://doi.org/10.1016/J.POLYMER.2004.01.057

Song, Y., Zhang, T., Song, X., Zhang, L., Zhang, C., Xing, J., & Liang, X. J. (2015). Polycations with excellent gene transfection ability based on PVP-g-PDMAEMA with random coil and micelle structures as non-viral gene vectors. *Journal of Materials Chemistry B*, *3*(5), 911–918. https://doi.org/10.1039/C4TB01754D

Srinivasa, P. C., Ramesh, M. N., Kumar, K. R., & Tharanathan, R. N. (2003). Properties and sorption studies of chitosan–polyvinyl alcohol blend films. *Carbohydrate Polymers*, *53*(4), 431–438. https://doi.org/10.1016/S0144-8617(03)00105-X

Stigter, M., Bezemer, J., De Groot, K., & Layrolle, P. (2004). Incorporation of different antibiotics into carbonated hydroxyapatite coatings on titanium implants, release and antibiotic efficacy. *Journal of Controlled Release : Official Journal of the Controlled Release Society*, *99*(1), 127–137. https://doi.org/10.1016/J.JCONREL.2004.06.011

Sullad, A. G., Manjeshwar, L. S., & Aminabhavi, T. M. (2010). Novel pH-Sensitive Hydrogels Prepared from the Blends of Poly(vinyl alcohol) with Acrylic Acid-graft-Guar Gum Matrixes for Isoniazid Delivery. *Industrial and Engineering Chemistry Research*, *49*(16), 7323–7329. https://doi.org/10.1021/IE100389V

Tripathi, A., Saravanan, S., Pattnaik, S., Moorthi, A., Partridge, N. C., & Selvamurugan, N. (2012). Bio-composite scaffolds containing chitosan/nano-hydroxyapatite/nano-copper-zinc for bone tissue engineering. *International Journal of Biological Macromolecules*, *50*(1), 294–299. https://doi.org/10.1016/J.IJBIOMAC.2011.11.013

Tsao, C. T., Leung, M., Yu-Fong Chang, J., & Zhang, M. (2014). A simple material model to generate epidermal and dermal layers in vitro for skin regeneration. *Journal of Materials Chemistry B*, *2*(32), 5256–5264. https://doi.org/10.1039/C4TB00614C

Uskokovič, V., & Desai, T. A. (2013). Phase composition control of calcium phosphate nanoparticles for tunable drug delivery kinetics and treatment of osteomyelitis. I. Preparation and drug release. *Journal of Biomedical Materials Research Part A*, *101A*(5), 1416–1426. https://doi.org/10.1002/JBM.A.34426

Uskoković, V., & Uskoković, D. P. (2011). Nanosized hydroxyapatite and other calcium phosphates: Chemistry of formation and application as drug and gene delivery agents. *Journal of Biomedical Materials Research Part B: Applied Biomaterials*, *96B*(1), 152–191. https://doi.org/10.1002/JBM.B.31746

Venkatasubbu, G. D., Ramasamy, S., Reddy, G. P., & Kumar, J. (2013). In vitro and in vivo anticancer activity of surface modified paclitaxel attached hydroxyapatite and titanium dioxide nanoparticles. *Biomedical Microdevices*, *15*(4), 711–726. https://doi.org/10.1007/S10544-013-9767-7/METRICS

Vino, A. B., Ramasamy, P., Shanmugam, V., & Shanmugam, A. (2012). Extraction, characterization and in vitro antioxidative potential of chitosan and sulfated chitosan from Cuttlebone of Sepia aculeata Orbigny, 1848. *Asian Pacific Journal*

*of Tropical Biomedicine*, *2*(1 SUPPL.). https://doi.org/10.1016/S2221-1691(12)60184-1

Vulic, K., & Shoichet, M. S. (2012). Tunable Growth Factor Delivery from Injectable Hydrogels for Tissue Engineering. *Journal of the American Chemical Society*, *134*(2), 882. https://doi.org/10.1021/JA210638X

Wang, S., Liu, R., Fu, Y., & Kao, W. J. (2020). Release mechanisms and applications of drug delivery systems for extended-release. *Https://Doi.Org/10.1080/17425247.2020.1788541*. https://doi.org/10.1080/17425247.2020.1788541

Wang, T., Zhu, X. K., Xue, X. T., & Wu, D. Y. (2012). Hydrogel sheets of chitosan, honey and gelatin as burn wound dressings. *Carbohydrate Polymers*, *88*(1), 75–83. https://doi.org/10.1016/J.CARBPOL.2011.11.069

Watanabe, K., Nishio, Y., Makiura, R., Nakahira, A., & Kojima, C. (2013). Paclitaxel-loaded hydroxyapatite/collagen hybrid gels as drug delivery systems for metastatic cancer cells. *International Journal of Pharmaceutics*, *446*(1–2), 81–86. https://doi.org/10.1016/J.IJPHARM.2013.02.002

Wilson, C. G., & Crowley, P. J. (2011). Controlled Release in Oral Drug Delivery. *Controlled Release in Oral Drug Delivery*. https://doi.org/10.1007/978-1-4614-1004-1

Wlodarski, K., Tajber, L., & Sawicki, W. (2016). Physicochemical properties of direct compression tablets with spray dried and ball milled solid dispersions of tadalafil in PVP-VA. *European Journal of Pharmaceutics and Biopharmaceutics*, *109*, 14–23. https://doi.org/10.1016/J.EJPB.2016.09.011

Wolkers, W. F., Oliver, A. E., Tablin, F., & Crowe, J. H. (2004). A Fourier-transform infrared spectroscopy study of sugar glasses. *Carbohydrate Research*, *339*(6), 1077–1085. https://doi.org/10.1016/j.carres.2004.01.016

Xu, B., Cao, Q., Zhang, Y., Yu, W., Zhu, J., Liu, D., & Jiang, G. (2018). Microneedles Integrated with ZnO Quantum-Dot-Capped Mesoporous Bioactive Glasses for Glucose-Mediated Insulin Delivery. *ACS Biomaterials Science & Engineering*, *4*(7), 2473–2483. https://doi.org/10.1021/ACSBIOMATERIALS.8B00626

Xu, Z., Liu, C., Wei, J., & Sun, J. (2012). Effects of four types of hydroxyapatite nanoparticles with different nanocrystal morphologies and sizes on apoptosis in rat osteoblasts. *Journal of Applied Toxicology*, *32*(6), 429–435. https://doi.org/10.1002/JAT.1745

Yang, Y. H., Liu, C. H., Liang, Y. H., Lin, F. H., & Wu, K. C. W. (2013). Hollow mesoporous hydroxyapatite nanoparticles (hmHANPs) with enhanced drug loading and pH-responsive release properties for intracellular drug delivery. *Journal of Materials Chemistry B*, *1*(19), 2447–2450. https://doi.org/10.1039/C3TB20365D

Ye, M., Kim, S., & Park, K. (2010). Issues in long-term protein delivery using biodegradable microparticles. *Journal of Controlled Release : Official Journal of the Controlled Release Society*, *146*(2), 241–260. https://doi.org/10.1016/J.JCONREL.2010.05.011

Yoo, C. Y., Seong, J. S., & Park, S. N. (2016). Preparation of novel capsosome with liposomal core by layer-by-Layer self-assembly of sodium hyaluronate and chitosan. *Colloids and Surfaces. B, Biointerfaces*, *144*, 99–107. https://doi.org/10.1016/J.COLSURFB.2016.04.010

Yun, Y. H., Lee, B. K., & Park, K. (2015). Controlled Drug Delivery: Historical perspective for the next generation. *Journal of Controlled Release*, *219*, 2–7. https://doi.org/10.1016/J.JCONREL.2015.10.005

Zhang, L., Liang, Y., Meng, L., & Wang, C. (2009). Characterization of complexation of PVP copolymer with DNA. *Polymers for Advanced Technologies*, *20*(4), 410–415. https://doi.org/10.1002/PAT.1288

Zhang, W., Zhao, Q., Deng, J., Hu, Y., Wang, Y., & Ouyang, D. (2017). Big data analysis of global advances in pharmaceutics and drug delivery 1980-2014. *Drug Discovery Today*, *22*(8), 1201–1208. https://doi.org/10.1016/J.DRUDIS.2017.05.012

Zheng, X., Zhang, T., Song, X., Zhang, L., Zhang, C., Jin, S., Xing, J., & Liang, X. J. (2015). Structural impact of graft and block copolymers based on poly(N-vinylpyrrolidone) and poly(2-dimethylaminoethyl methacrylate) in gene delivery. *Journal of Materials Chemistry B*, *3*(19), 4027–4035. https://doi.org/10.1039/C4TB01956C

Zhu, Y., Lu, W., Guo, Y., Chen, Y., Wu, Y., & Lu, H. (2018). Biocompatible, stretchable and mineral PVA-gelatin-nHAP hydrogel for highly sensitive pressure sensors. *RSC Advances*, *8*(65), 36999–37007. https://doi.org/10.1039/C8RA06193A

Zidan, H. M., Abdelrazek, E. M., Abdelghany, A. M., & Tarabiah, A. E. (2019). Characterization and some physical studies of PVA/PVP filled with MWCNTs. *Journal of Materials Research and Technology*, *8*(1), 904–913. https://doi.org/10.1016/J.JMRT.2018.04.023

Zulfiqar, M., Lee, S. Y., Mafize, A. A., Kahar, N. A. M. A., Johari, K., & Rabat, N. E. (2020). Ecient removal of PB(II) from aqueous solutions by using oil palm bio-waste/MWCNTs reinforced pva hydrogel composites: Kinetic, isotherm and thermodynamic modeling. *Polymers*, *12*(2). https://doi.org/10.3390/polym12020430

# CURRICULUM VITEA

Batool ALMAFRACHI holds a bachelor’s degree in materials science and Engineering Department, Faculty of Engineering, Mustansiriyah University, Baghdad, Iraq. In 2020, I started my Master's program at the Ondokuz Mayıs University, Institute of Graduate Studies, Nanoscience and Nanotechnology Department. Samsun, Turkey.

**Contact information**

ORCID ID: 0000-0001-5923-3763

**Publications**

ALMAFRACHI, Batool. ANDAÇ, Ömer. 2022. “Synthesis and Characterization of Chitosan/Poly(vinyl alcohol)/Poly(vinylpyrrolidone) Hydrogels for Biomedical Application”. 2nd International Congress on Scientific Advances (ICONSAD'22). Turkey.